

2003

Cell Biology Of ApoE In Cortical Cultured Neurons: Possible Roles In Alzheimer's Disease

Anna G. Barsukova

Eastern Illinois University

This research is a product of the graduate program in [Biological Sciences](#) at Eastern Illinois University. [Find out more](#) about the program.

Recommended Citation

Barsukova, Anna G., "Cell Biology Of ApoE In Cortical Cultured Neurons: Possible Roles In Alzheimer's Disease" (2003). *Masters Theses*. 1425.
<https://thekeep.eiu.edu/theses/1425>

This is brought to you for free and open access by the Student Theses & Publications at The Keep. It has been accepted for inclusion in Masters Theses by an authorized administrator of The Keep. For more information, please contact tabruns@eiu.edu.

THESIS/FIELD EXPERIENCE PAPER REPRODUCTION CERTIFICATE

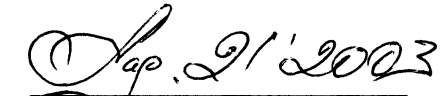
TO: Graduate Degree Candidates (who have written formal theses)

SUBJECT: Permission to Reproduce Theses

The University Library is receiving a number of request from other institutions asking permission to reproduce dissertations for inclusion in their library holdings. Although no copyright laws are involved, we feel that professional courtesy demands that permission be obtained from the author before we allow these to be copied.

PLEASE SIGN ONE OF THE FOLLOWING STATEMENTS:

Booth Library of Eastern Illinois University has my permission to lend my thesis to a reputable college or university for the purpose of copying it for inclusion in that institution's library or research holdings.


Date

I respectfully request Booth Library of Eastern Illinois University **NOT** allow my thesis to be reproduced because:

Author's Signature

Date

Cell Biology Of ApoE In Cortical Cultured Neurons
- Possible Roles In Alzheimer's Disease

BY

Anna G. Barsukova

THESIS

SUBMITTED IN PARTIAL FULFILLMENT OF THE REQUIREMENTS
FOR THE DEGREE OF

MASTER IN BIOLOGICAL SCIENCES

IN THE GRADUATE SCHOOL, EASTERN ILLINOIS UNIVERSITY
CHARLESTON, ILLINOIS

2003
YEAR

I HEREBY RECOMMEND THAT THIS THESIS BE ACCEPTED AS FULFILLING
THIS PART OF THE GRADUATE DEGREE CITED ABOVE

08/20/03
DATE

8/21/03
DATE

ABSTRACT

The apolipoprotein E4 (apoE4) genotype is a major risk factor for Alzheimer's disease (AD). Previous studies have shown that apoE4 is less effective than apoE3 in supporting neurite outgrowth in adult mice cortical cultures. However the mechanism underlying this phenomenon is not known. To understand this mechanism and the broader role of apoE isoforms on neuronal biology I examined the rate of apoE isoforms internalization in neurons, effects of apoE isoforms on lipid uptake by neurons, effects of apoE isoforms on neuronal environment – microglia and on neuroregeneration, or neurogenesis.

I examined the binding and internalization of recombinant human apoE3 and apoE4 in cortical cultures derived from adult apoE knockout mice. The cultures were incubated with apoE3 or apoE4 over various time periods at temperatures between 4°C and 37°C before immunocytochemistry for apoE was performed. The data revealed that cell-associated apoE3 uptake was significantly greater ($\cong 2.5$ times) than apoE4 regardless of the incubation time; the percent of total immunoreactivity in the cell body compared to dendritic immunoreactivity declined in the apoE3 group but did not change in the apoE4 group primarily because of increased total apoE per neuron.

To determine the lipoprotein receptors that mediate the differential uptake of apoE3 and apoE4 in neurons, I blocked the low-density lipoprotein (LDL) receptor related protein (LRP) and cell surface heparan sulfate proteoglycans (HSPG). The data revealed that inhibition of LRP decreased both apoE3 and apoE4 uptake. Blocking HSPG totally inhibited uptake to undetectable levels. The data suggests that HSPG has a pivotal role in apoE internalization.

I predicted that apoE3 would deliver more lipids to neurons than apoE4 because the rate of uptake of apoE3 was faster than apoE4 in neurons. To test this hypothesis, I examined fluorescently labeled dodecanoic acid accumulation in adult cortical neurons. Cells cultured with apoE3 internalized approximately twice as much vesicular accumulations of fluorescence as those with apoE4. ApoE4 roughly doubled the amount of lipid internalized compared to the absence of apoE. Therefore, although apoE4 was better than no apoE, it was less effective than apoE3 in providing lipids.

Previous studies demonstrated that apoE regulates microglial activation and inducible nitric oxide synthase (iNOS) in embryonic and postnatal mouse microglial cultures. I examined and compared the effects of apoE3 and apoE4 on microglial proliferation, morphology and activation in adult mouse cortical (AMC) and adult mouse microglial (AMM) cultures. Microglial proliferation and morphology for each apoE treatment in AMC and AMM cultures were assessed by immunocytochemistry; levels of iNOS expression were assessed by immuno-blotting. The results from this study demonstrated that apoE3 and apoE4 differentially regulate microglial proliferation and activation and iNOS production in a neuron-microglia independent manner and apoE4 induces microglial proliferation and activation, when compared to apoE3.

Recent findings concerning the regenerative potential of the adult brain showed that adult neurons have the ability to divide, a process known as neurogenesis. I examined the effects of apoE3 and apoE4 on neurogenesis in AMC culture. Neuronal proliferation in apoE3 or apoE4 treated cells was analyzed with MTT and BrdU cell proliferation kits, followed by ELISA and immunocytochemistry. The results show that the fraction of neurons in the DNA synthesis stage to total number of neurons in apoE3

treatment was significantly higher than in apoE4 and apoE KO treatment groups. These data suggests that apoE4 is less efficient in promoting neurogenesis. This study also revealed new phenomenon of BrdU-positive satellite stain outside the BrdU-positive nucleus in approximately 50% of dividing neurons. The significance of the satellite BrdU-positive stain found in adult neurons in both apoE isoform treatment groups is yet to be determined.

DEDICATION

I would like to thank my mentor Dr. Britto Nathan for his teaching, his knowledge, his support and patience, for giving me the opportunity to perform this extraordinary interesting and important research, for always being there for me with advise and help, for believing in me and my ideas and for encouraging me to explore more with every passing day.

I would like to thank Dr. Kipp Kruse and Dr. Charles Costa, my graduate committee members, for their teaching and support, for always being there for me with advise and help and for giving me the opportunity to participate in leading conferences on Neuroscience and Alzheimer's disease last year.

I would like to thank my fellow students: Melissa Litherland, Jennifer Pritts, Nick Short, Elin Grissom, Emily Rozario, Fei Shen, Matt Kircher and Paul Mcadamis for two wonderful years of research and study together, for their support, knowledge and friendship.

I would like to thank the whole Department of Biological Sciences for the two wonderful years of working and learning from all within the Department. I am very privileged to be a part of Biological Sciences at EIU and I am very grateful for all the knowledge that I received and for the friendships. I promise to take this knowledge to as far as I can and make all within our Department proud.

I would like to thank the Graduate School and International Programs at EIU for giving me this unique opportunity for graduate study, research and for reaching new heights in my academic career in contributing to the field of Neuroscience. Specifically I

would like to thank Dr. Robert Augustine, Sue Songer, Marilyn Thomas and Adrienne Paladino.

I especially would like to thank my parents for teaching me, starting at the very young age, that knowledge and learning are two of the most precious gifts in life, for their love and support, for believing in me, for always being there for me with a word of advice and encouragement.

And, finally, I would like to thank my best friend and my special person, Ken Gerhardt, for his love, friendship and support, for helping me tremendously in these two years of my study, research and for helping our whole laboratory with his professional advice.

ACKNOWLEDGMENTS

I would like to thank Dr. Scott Meiners (Biological Sciences, EIU) and Dr. Robert Struble (Center for Alzheimer Disease and Related Disorders, Southern Illinois University School of Medicine) for their assistance with statistical analysis.

I would like to thank Dr. Gene Wong (Biological Sciences, EIU) for his assistance and advice on imaging and image analysis techniques.

I would like to thank Dr. Scott Meiners and Dr. Steve Daniel (Biological Sciences, EIU) for their assistance and advice on Power Point presentations and poster creation.

I would like to thank Dr. Jeff Laursen for his assistance with ELISA technique and protocols.

TABLE OF CONTENTS

	Page
List of Figures.....	9-10
1. Introduction.....	11-15
2. Methodology.....	16-26
3. Results.....	27-50
4. Discussion.....	51-63
5. Conclusions	64-65
6. Bibliography	66-69

LIST OF FIGURES

		Page
Figure 1.	Fractions of cell types in the adult mouse cortical culture	28
Figure 2.	Representative morphologies of immuno-stained cells in adult mouse cortical culture	28
Figure 3.	Quantification of cellular accumulation of apoE3 and apoE4 at 5, 15, 30, 60 min at 37°C and at 60 min at 4°C in adult mouse cortical neurons	29
Figure 4.	Cellular accumulation of apoE3 and apoE4 at 5, 15, 30, 60 min at 37°C and at 60 min at 4°C in adult mouse cortical neurons	30
Figure 5.	Quantification of cellular accumulation of apoE3 in somata and dendrites at 5, 15, 30, 60 min at 37°C and at 60 min at 4°C in adult mouse cortical neurons	31
Figure 6.	Quantification of cellular accumulation of apoE4 in somata and dendrites at 5, 15, 30, 60 min at 37°C and at 60 min at 4°C in adult mouse cortical neurons	32
Figure 7.	Quantification of apoE3 and apoE4 in adult mouse cortical neurons following LRP-HSPG inhibition	33
Figure 8.	Accumulation of apoE3 and apoE4 in adult mouse cortical neurons following LRP-HSPG inhibition	34
Figure 9.	Quantification of fatty acid uptake mediated by apoE3 and apoE4 in adult mouse cortical neurons	35
Figure 10.	Fatty acid uptake facilitated by apoE3 and apoE4 in adult mouse cortical neurons	36
Figure 11.	Quantification of the effect of apoE3 and apoE4 on microglial proliferation in adult mouse cortical culture	37
Figure 12.	Quantification of the effect of apoE3 and apoE4 on microglial morphology in adult mouse cortical culture	38
Figure 13.	Effect of apoE3 and apoE4 on microglial morphology in adult mouse cortical culture	39

Figure 14.	Quantification of the effect of apoE3 and apoE4 on microglial proliferation in adult mouse microglial culture	40
Figure 15.	Quantification of the effect of apoE3 and apoE4 on microglial morphology in adult mouse microglial culture	41
Figure 16.	Effect of apoE3 and apoE4 on microglial number and morphology in adult mouse microglial culture	42
Figure 17.	Quantification of iNOS production in response to apoE3 and apoE4 in adult mouse cortical culture	43
Figure 18.	Effect of apoE3 and apoE4 on iNOS production in AMC culture in adult mouse cortical culture	44
Figure 19.	Quantification of cell proliferation in adult mouse cortical culture in response apoE3 and apoE4 by ELISA	45
Figure 20.	Quantification of the number of neurons in adult mouse cortical culture in response to apoE3 and apoE4	46
Figure 21.	BrdU and β -tubulin immunocytochemistry in adult mouse cortical culture	47
Figure 22.	BrdU-positive neurons in adult mouse cortical culture treated with apoE3, apoE4 or no apoE (apoE KO)	48
Figure 23.	Effect of apoE3 and apoE4 on neurogenesis in adult mouse cortical culture	49
Figure 24.	BrdU-staining satellite cell phenomenon in dividing adult neurons in adult mouse cortical culture	50

1. INTRODUCTION

Apolipoprotein (apo-) E, a 34,000 kDa protein, exists in three major isoforms (apoE2, apoE3 and apoE4) that are produced by three alleles (e2, e3 and e4, respectively) at a single gene locus on chromosome 19 in humans [1]. The most common isoform, apoE3, has cysteine and arginine at position 112 and 158, respectively [2]. Both positions contain cysteine in apoE2 and arginine in apoE4. ApoE serves to distribute lipids among tissues and cells by carrying the hydrophobic lipids and binding to lipoprotein receptors on the cell surface [3]. Binding of apoE to the receptor results in internalization of lipoproteins (lipids + apoE) by receptor-mediated endocytosis. Through its function in transporting lipids among cells, apoE plays a critical role in lipid metabolism within the body, including the CNS.

Recent findings demonstrate that inheritance of the e4 allele of apoE increases the risk of Alzheimer's disease (AD) [4]. The mechanism by which apoE4 contributes to AD is unknown. Previous research has demonstrated that apoE3 promotes neurite outgrowth in adult mouse cortical (AMC) neurons, whereas apoE4 inhibits neurite outgrowth [5]. A better understanding of the pathway by which apoE isoforms enter the cell and how they accumulate in neurons overtime was the aim of my first study on role of apoE4 in AD.

I examined the binding and internalization of recombinant human apoE3 and apoE4 in cortical cultures derived from adult apoE knockout mice. The data revealed that cell-associated apoE3 was significantly greater ($\cong 2.5$ times) than apoE4 regardless of the incubation time. The percent of total immunoreactivity in the cell body compared to dendritic immunoreactivity declined in the apoE3 group but did not change in the

apoE4 group primarily because of increased total apoE per neuron. No significant differences in cell associated apoE3 or apoE4 was detected in cultures incubated at 4°C.

To determine the lipoprotein receptor that mediates the differential uptake of apoE3 and apoE4 in neurons, I blocked the low-density lipoprotein (LDL) receptor related protein (LRP). The data revealed that inhibition of LRP with the receptor associated protein (RAP) (5 µg/ml) and lactoferrin (LAC) (10 µg/ml) decreased both apoE3 and apoE4 uptake. The role of heparan sulfate proteoglycans (HSPG), which are necessary for the binding of apoE enriched lipoproteins to the cells prior to internalization via the LRP, was examined by removing HSPG with heparinase (10 units/ml). Heparinase treatment totally inhibited uptake to undetectable levels. Uptake inhibition by both RAP and LAC confirms the importance of the LRP in this response and suggests that HSPG has a pivotal role in apoE internalization.

I predicted that apoE4 would deliver fewer lipids to neurons than apoE3 because the rate of uptake of apoE4 was slower than apoE3 in neurons. To test this hypothesis, I examined fluorescently labeled dodecanoic acid accumulation in adult cortical neurons. Cells cultured with apoE3 internalized approximately twice as much vesicular fatty acid as those with apoE4. ApoE4 roughly doubled the amount of lipid internalized compared to the absence of apoE. Therefore, although apoE4 was better than no apoE, it was much less effective than apoE3 in providing lipids.

Glia are present in significant numbers in the early stages of culture. This is important to note, since previous data suggest that glia are a primary source of apoE [6]. To identify glia, I previously [5] performed immunocytochemistry to label neurons (β-tubulin), astroglia (glial fibrillary acidic protein) or lectin binding to label microglia

(BSL1). At 3 days *in vitro* (DIV) I found that neurons comprise 70% of total cells, astroglia 15% and microglia 15%.

Many recent studies have focused on the role of microglia in pathogenesis of AD [7, 8, 9, 10,]. Results of several genetic studies showed a significant increase in amyloid plaques in AD patients with allele $\epsilon 4$ of apoE [11,12] and that plaques in AD patients are surrounded by activated microglia and reactive astrocytes [13]. Microglia respond to damage or infection by proliferation and changing the morphology to macrophage-like phagocytic cells [15]. Results from recent study have indicated that microglial activation was induced in primary microglial cell cultures by factors contained in sera of AD-related apoE 3/4 and apoE 4/4 genotypes [14]. However, previous studies used embryonic and postnatal neuronal cultures to examine the effect of factors contained in sera of AD-related apoE genotypes.

The aim of my next study was to determine the role of recombinant human apoE3 and apoE4 isoforms on cellular biology of microglia in two models: adult mouse cortical culture (AMC) and adult mouse microglial culture (AMM). The questions this study sought to answer were: (1) Do purified human apoE isoforms differentially effect microglial number and activation in AMC culture? (2) Is this effect mediated via neuron-glia interaction or do human apoE isoforms have a direct effect on microglial activation and number?

Microglial activation is characterized by increase in microglial proliferation, inducible nitric oxide synthase production and change in microglial morphology to amoeboid phagocytic cells. ApoE KO adult mouse cortical (AMC) and apoE KO adult mouse microglial (AMM) cultures were treated with recombinant human apoE3 and

apoE4 (3 µg/ml), respectively, for 2 consecutive days, following by treatment with LPS (100 ng/ml) to stimulate inducible nitric oxide synthase (iNOS) production in each apoE treatment group. Microglial proliferation and morphology for each apoE treatment in AMC and AMM cultures were assessed by immunocytochemistry; levels of iNOS expression were assessed by immuno-blotting. The results from this study demonstrate that (1) apoE KO AMC and AMM cultures have the highest number of microglia with macrophage-like morphology and highest iNOS levels, when compared to apoE3 and apoE4 treatments; (2) apoE3 and apoE4 differentially regulate microglial number, activation and iNOS production; (3) apoE3 decreased microglial proliferation, activation and iNOS production in both AMC and AMM cultures by nearly 60%, whereas apoE4 by only 20%, as compared to apoE KO AMC and AMM cultures. These data show that apoE isoforms regulate microglial proliferation and activation in a neuron-microglia independent manner and apoE4 up-regulates microglial proliferation and activation, as compared to apoE3.

Although the mammalian brain has long been thought to be entirely post mitotic, the recent discoveries have confirmed an existence of adult neuronal division and neural progenitor cells in various regions of the adult mammalian brain [16,17,18]. These recent findings, concerning the regenerative potential of the adult brain, showed that neurogenesis takes place in adult olfactory bulb, adult retina and the hippocampus. In the past two years of my research, neurogenesis was observed in AMC cultures at 3 and 4 DIV.

In the present study I examined the effects of apoE3 and apoE4 on neurogenesis in AMC culture. ApoE KO AMC cultures were treated with recombinant human apoE3

and apoE4 (3 µg/ml), respectively, for 2 consecutive days. On day 3 the number of cells in AMC culture, treated with either apoE3 or apoE4 were analyzed by MTT cell proliferation kit, followed by ELISA. The number of neurons was determined by immunocytochemistry for neuron specific β -tubulin. The number of neurons in the stage of DNA synthesis was determined by double immunocytochemistry with anti- β -tubulin and BrdU stain. Study of the effect of apoE3 and apoE4 on neurogenesis in AMC culture showed that there was a significant difference in the number of neurons in the DNA synthesis stage by day 4 in AMC culture. Percent of BrdU-positive neurons to total number of neurons in the random field in apoE3 treatment was significantly higher than percent of BrdU-positive neurons in apoE4 and apoE KO treatment groups. This study also revealed new phenomena of BrdU-positive satellite stain in approximately 50% of dividing neurons. The stain appears to correspond to an undifferentiated cell in the dendritic tree or at perikaryon of a dividing neuron. The significance of the satellite BrdU-positive stain found in adult neurons in both apoE isoform treatment groups and in apoE KO treatment should be further determined.

Based on the results from the four areas of my study, I propose that apoE4 is less effective than apoE3 in binding and accumulating in neurons, delivering lipids to adult neurons, suppressing microglial activation and promoting neurogenesis in adult brain. Taken together, these data suggests that apoE4 may have several effects on adult neurons and neuronal environment that lead to poor neuronal growth, repair, proliferation, thus playing a possible role in age-related diseases including AD.

2. METHODOLOGY

2.1. Materials

2.1.1. *Adult mouse cortical culture and microglial cultures*

Homozygous apoE KO mice (C57BL/6-Apoe^{<tm1Unc>}, Cat. # 002052) bred 10 generations onto the C57BL/6 background were obtained from Jackson Laboratory (Bar Harbor, ME). Cell culture medium, including Hibernate A (Cat. # 10740-025), Neurobasal (Cat. # 21103-049), and B27 medium supplement (Cat. # 17504-010) were purchased from Life Technologies Inc., (Gaithersburg, MD). Glutamine (Cat. # G-3126) and poly-D-lysine (Cat. # P-6407) were purchased from Sigma Chemicals (St. Louis, MO). Papain (Cat. # 3119) was obtained from Worthington (Lakewood, NJ). Gentamicin (Cat. # 15710-015), FGF2 (Cat. # 13256-029), and Optiprep (Cat. # 103-0061) were from Life Technologies Inc., (Gaithersburg, MD). Twelve-millimeter glass cover slips (Cat. # P7-63-3029) were purchased from Carolina Biological (Burlington, NC). Falcon Brand 35 mm diameter dishes (Cat. # 08-772-4A) and Costar Brand Tissue Culture 24-well plates (Cat. # 07-200-84) were purchased from Fisher Scientific (Chicago, IL).

2.1.2. *Immunocytochemistry for neurons, astrocytes and microglia*

The mouse Anti-beta III Tubulin mAb (Cat. # G7121) was obtained from Molecular Probes, mouse anti-Glial Fibrillary Acidic Protein (GFAP) (Cat. # N-3893), and FITC- or TRITC-conjugated lectin from *Bandeiraea simplicifolia* (BSL-1) were obtained from Sigma Chemicals (St. Louis, MO). The FITC- or TRITC-conjugated goat

anti-mouse IgG-Fab₂ specific (Cat. # 115-095-006) and normal goat serum (Cat. # 005-000-121) were purchased from Jackson ImmunoResearch (West Grove, PA). Triton X-100 (Cat. #T-9284) was purchased from Sigma Chemicals (St. Louis, MO). Anti-photobleach was purchased from Vectorshield Co.

2.1.3. Human ApoE

Human recombinant apoE3 (Cat. # P2003) and apoE4 (Cat. # P2004) were purchased from Panvera (Madison, WI), and dialyzed overnight in 0.1M ammonium bicarbonate.

2.1.4. Immunocytochemistry for apoE

Goat anti-human apoE (Cat. # 178479) was purchased from Calbiochem (San Diego, CA). FITC-conjugated secondary antibody, and rabbit anti-goat IgG (Cat. # 305-006-003) was obtained from Jackson ImmunoResearch (West Grove, PA).

2.1.5. ApoE quantification

The monoclonal anti-apoE (3H1) used for immunoprecipitation was obtained from the University of Ottawa, Heart Institute. HRP conjugated secondary antibody, and rabbit anti-goat IgG (Cat. # AP106P) was obtained from Chemicon (Temecula, CA). Protein A-Sepharose CL-4B (Cat. # P-3391) and BSA (Cat. # A-9418) were obtained from Sigma Chemicals (St. Louis, MO). Goat anti-human apoE (Cat. # 178479) was purchased from Calbiochem (San Diego, CA). All other materials used for apoE quantification, including pre-cast 4-20% gradient gels (Cat. # FB3435), Millipore Immobilon-P Transfer

Membranes (Cat. # IPVH00010), Pierce SuperSignal West Pico Chemiluminescent Substrate (Cat. # PI34080), Kodak BioMax Light-2 film (5*7', Cat. # 05-728-53), Tris (Cat. # BP154-1), Glycine (Cat. # BP381-1), SDS (Cat. # BP166-100), Tween 20 (Cat. # BP337-500) and sodium bromophenol blue (Cat. # BP-114-25) were purchased from Fisher Scientific (Chicago, IL).

2.1.6. LRP-HSPG inhibition

Heparinase I (Cat. # 51539) was purchased from and lactoferrin (Cat. # L9507) was purchased from Sigma Chemicals (St. Louis, MO), RAP was kindly provided by Dr. Dudley Strickland from American Red Cross (MD).

2.1.7. Fatty acid

4,4-difluoro-5-methyl-4-bora-3a,4a-diaza-s-indacene-3-dodecanoic acid (C₁-BODIPY® 500/510 C₁₂) (Cat. # D-3823) was purchased from Molecular Probes (Eugene, OR).

2.1.8. iNOS quantification

Bacterial lipopolysaccharide (LPS) from *Salmonella typhimurium* (Cat. # L9516) and monoclonal anti-nitric oxide synthase inducible antibody (Cat. # N9657) was purchased from Sigma Chemicals (St. Louis, MO). Horseradish peroxidase-conjugated goat anti-mouse IgG-Fab₂ (Cat. # AP308P) was purchased from Chemicon (Temecula, CA).

2.1.9. Cell proliferation and neurogenesis

Cell Proliferation Kit I (MTT-based) (Cat. # 1465007) and In Situ Cell Proliferation Kit FLUOS (Cat. # 1810740) were obtained from Roche Applied Science (Indianapolis, IN).

2.2. Methods

2.2.1 Adult mouse cortical culture

Techniques for the *in vitro* culture of neurons from adult mice were modified as previously described [19]. For each experiment, a four-month-old mouse was anesthetized with sodium pentobarbital (80 mg/kg). The entire cerebral cortex was dissected from the rest of the brain in 2 ml B27/Hibernate A medium [B27/Hibernate A with 0.5 mM glutamine] in a 35 mm diameter Petri dish at 4°C. The cortex was sliced (0.5 mm thickness) and transferred to a 50 ml tube containing 5 ml B27/Hibernate A medium. After warming for 8 min at 30°C, slices were digested with 6 ml of a 2 mg/ml Papain solution in Hibernate A for 30 min at 30°C in a gyrating water bath to keep the slices suspended. Slices were transferred to 2 ml B27/Hibernate A medium in a 15 ml tube. After 2 min at room temperature, slices were triturated 10 times with a siliconized 9-inch Pasteur pipette, and allowed to settle for 1 min. Approximately 2 ml of the supernatant was transferred to another tube, and the sediment resuspended in 2 ml B27/Hibernate A medium. The above step was repeated twice, and a total of 6 ml collected. The resultant supernatant was subjected to density gradient centrifugation at 800g for 15 min. The density gradient was prepared in four 1 ml steps of 35, 25, 20 and

15% Optiprep in B27/Hibernate A medium (v/v). The fraction containing the neurons was collected, and diluted in 5 ml B27/Hibernate A medium. After centrifuging twice at 200g for 2 min, the cell pellets were resuspended in 3 ml B27/Neurobasal A medium [B27/Neurobasal A with 0.5 mM glutamine, no glutamate, 0.01 mg/ml gentamicin]. Suspended cells were counted in a hemacytometer, and 40,000 cells were plated in 50 μ l aliquots on glass cover slips (12 mm diameter) previously coated overnight with 100 μ l of 50 μ g/ml poly-D-lysine in water. Following 1 hr incubation in a humidified incubator at 37 °C and 5% CO₂, cover slips were transferred to a 24-well plate containing 0.4 ml B27/Neurobasal A medium. Cover slips were rinsed twice with B27/Hibernate A medium, and then 0.4 ml growth medium [B27/Neurobasal A medium with 5 ng/ml FGF2] was added to each well and the plate was further incubated. Neurite outgrowth, and viability assays were performed after 4 days of incubation, as described below. For culture periods greater than 4 days, half of the medium was replaced with B27/Neurobasal A with 10 ng/ml FGF2 every four days.

2.2.2. Immunocytochemistry

Cells from 4-day old cultures were rinsed with warm PBS (37°C) and fixed with 4% paraformaldehyde in PBS for 20 min at room temperature. After rinsing twice with PBS, cells were permeabilized with 0.5% Triton X-100 in PBS for 5 min. Cells were rinsed again with PBS, and then blocked with 5% normal goat serum, 0.05% Triton X-100 in PBS for 1 hr. Cells were incubated at room temperature for 2 hours with anti- β -tubulin 1 μ g/ml in PBS, or mouse anti-GFAP (1:200) in the blocking solution. After rinsing four times with PBS, cells were incubated with FITC-conjugated goat anti-mouse IgG-Fab₂

(1:200) in blocking solution for 60 min. Cells were washed four times in PBS, slips were mounted in anti-photobleach medium (0.85 M n-propyl gallate, 60% glycerol in TBS). Immuno-reactive cells were counted and digitally photographed on an Olympus BX50 microscope with appropriate fluorescence excitation filters.

For BSL1 labeling of microglia, cells were fixed as described above, rinsed with warm PBS, and incubated with fluorescein conjugated BSL1 (1:100 dilution) for 30 min at room temperature. Following incubation the cells were rinsed with PBS, and fixed with 4% paraformaldehyde in PBS for 5 min. After rinsing in PBS, slips were mounted with anti-photobleach and immuno-fluorescence was evaluated by fluorescence microscopy using 400× and 1000× magnification.

2.2.3. ApoE and apoE/ β -tubulin immunocytochemistry

At 3 DIV growth medium was removed and only 200 μ l of the medium was replaced. Cells were incubated for 1 hour at 37°C in the humidified incubator with 5% CO₂. ApoE3 and apoE4 isoforms of human apoE were added to the wells to reach final concentration of 3 μ g/ml. Cells were incubated for 5, 15, 30 and 60 minutes in the incubator at 37°C and for 60 minutes at 4°C. No ApoE was added to the control wells. Following the incubation with apoE3 and apoE4, cover slips were rinsed 3 times with 37°C T-TBS (20 mM Tris-HCl, 150 mM NaCl, 0.05% Tween 20, pH 7.5) and then washed in T-TBS three times for 5 min. Cover slips were washed with 30% ethanol in T-TBS for 10 min and fixed in 80% ethanol for 1 hour at room temperature. Cover slips were rinsed again with T-TBS 3 times, permeabilized with 0.5% Triton X-100 in T-TBS for 30 min and rinsed 3 times with T-TBS. Non-specific blocking was performed using

1% BSA, 15% apoE KO mouse serum in T-TBS for 1 hour and 10 minutes at room temperature, after which cover slips were rinsed 3 times in T-TBS. Cells were incubated with primary antibody (anti-apoE human, goat) 1:200 in T-TBS at room temperature for 2 hours and then rinsed with T-TBS, washed 3 times for 10 minutes in T-TBS and rinsed once more. Cells were incubated with secondary antibody (FITC conjugated donkey anti-goat), 1/200 in T-TBS for 30 min at RT, in the dark. Cover slips were finally rinsed with T-TBS, washed 3 times in T-TBS for 5 min and washed again 2 times for 5 minutes in distilled water, covered from light and mounted on the microscope slide with anti-photobleach. Double immunocytochemistry for apoE and β -tubulin was performed by co-incubation with anti-apoE human, goat, 1:200 and 1 μ g/ml anti- β -tubulin in PBS for 2 hours at RT; followed by FITC conjugated donkey anti-goat 1:200 for 30 min and TRITC donkey anti-goat 1:200 for 50 minutes. Cover slips were mounted with anti-photobleach and sealed. Immuno-fluorescence was evaluated by fluorescence microscopy using 400 \times magnification.

2.2.4. Fatty acid immunocytochemistry

At 3 DIV AMC culture was co-incubated with 4,4-difluoro-5-methyl-4-bora-3a, 4a-diaza-s-indacene-3-dodecanoic acid (10 μ g/ml) and apoE3 or apoE4 (3 μ g/ml) for 1 hr in humidified atmosphere (37°C, 5% CO₂). Cells were washed 3 times with warm PBS and the cover slips were mounted in PBS on microscope slides. Immuno-fluorescence was evaluated by fluorescence microscopy in live cells using 100 \times objective.

2.2.5. Adult mouse microglial culture

The cells were initially prepared as described above in Methods 2.2.1. including the first density gradient spin step. The density gradient separates the cortex into cell layers, where microglia can be found at the bottom of the tube in the form of a small pellet [19]. After the density gradient spin as described in Methods 2.2.1, the pellet was collected and spun twice with 5 ml of B27/Hibernate A medium. Cells were resuspended in 1 ml of B27/Neurobasal A medium, counted in a hemacytometer, and 40,000 cells were plated in 150 μ l aliquots on untreated glass cover slips (12 mm diameter) for 30 minutes in a humidified incubator at 37 °C and 5% CO₂. Then cell were gently rinsed once with warm B27/Neurobasal A medium and 0.4 ml growth medium [B27/Neurobasal A medium with 5 ng/ml FGF2] was added to each well and the plate was further incubated.

2.2.6. Stimuli

Bacterial lipopolysaccharide (LPS) from *Salmonella typhimurium* was used to stimulate inducible nitric oxide synthase (iNOS) production by activated microglia in AMC and AMM cultures. LPS was resuspended in sterile PBS at 10 mg/ml and was added to AMC culture medium at final concentration of 100 ng/ml on 4 DIV, 12 hours prior to fixing.

2.2.7. iNOS quantification

Cell medium from 3 wells (1200 μ l) per apoE treatment from 4-day-old AMC cultures was collected and centrifuged to eliminate suspended cells. iNOS was immunoprecipitated by incubating the supernatant with 1.2 μ l of monoclonal anti-NOS antibody on ice for 1 hour. Following incubation, 12 μ l of 10% protein A-Sepharose CL-4B was added, and the medium was further incubated on ice for 1 h on a shaker. The

medium was centrifuged at 10 000 g for 15 min at 4 °C and the supernatant discarded. The pellet was boiled for 5 min in 2× Lammeli sample buffer and electrophoresed on 4-20% SDS-polyacrylamide gradient gels in EC120 Mini gel vertical system. The samples were run at 80 V until separation began, and then at 120 V until the dye front neared the bottom of the gel.

Following electrophoresis, the gel was placed in transfer buffer (3.03 g Tris base, 14.4 g glycine, 200 ml methanol, 800 ml distilled H₂O, pH 7.6) on a shaker for 10 min. The transfer membrane, Millipore Immobilon-P Transfer Membrane, was first soaked in methanol for 5 s and then washed in distilled H₂O for 5 min to remove excess methanol. The proteins in the gel were transferred to the Immobilon-P membrane using a Bio-Rad Trans-blot Transfer Cell following the manufacture's protocol.

Blots were blocked in PBS buffer with 3% dry non-fat milk for 20 min at room temperature on a shaker. The blots were incubated with monoclonal anti-NOS inducible antibody 1:1000 in PBS buffer with 3% dry non-fat milk on a shaker at 4 °C overnight. Then blots were washed 6 times (10 min each) in TBS-T buffer (20 mM Tris-HCl, 150 mM NaCl, 0.05% Tween 20, pH 7.5). Blots were then incubated in HRP-conjugated goat anti-mouse IgG 1:2 000 dilution in PBS buffer with dry non-fat milk for 1.5 h on a shaker at room temperature, washed 6 times (10 min each) with TBS-T buffer, incubated with Pierce SuperSignal West Pico Chemiluminescent Substrate, and then exposed to Kodak BioMax Light-2 film. A 130-kDa band were visualized which is consistent with the published molecular weight of NOS. Bands were quantified by densitometry (Scion Image, MD, USA).

2.2.8. Cell proliferation and ELISA

The assay is based on the cleavage of the yellow tetrazolium salt MTT to purple formazan crystals by metabolic active cells. The formazan crystals formed are solubilized and the resulting colored solution is quantified using a scanning multiwell spectrophotometer (ELISA reader). AMC cultures was grown in 100 μ l of Neurobasal A supplemented with B27 in a 96 well tissue culture plates. At 3 DIC the MTT labeling reagent 0.5 mg/ml was added to each well. The plates were incubated for 4 h in a humidified atmosphere (37°C, 5% CO₂). Solubilization solution (20 μ l) was then added into each well. Plates were incubated overnight in a humidified atmosphere (37°C, 5% CO₂). Spectrophotometrical absorbance of the samples was measured using a microtiter plate (ELISA) reader at 562 nm.

2.2.9. BrdU/ β -tubulin immunocytochemistry

At 3 DIV 40 μ l of BrdU labeling solution was added to the culture medium containing no FGF and cells were incubated for 60 min at 37°C in a humidified atmosphere (5% CO₂). The cover slips were washed 3 times in PBS and fixed with the In Situ Proliferation Kit FLOUS kit fixative solution for 45 min at RT. Cover slips were then washed 2 times in PBS, 2 \times 2 min, at RT and incubated in denaturation solution (4 M HCl) for 20 min, at RT. Cells were neutralized in PBS 3 \times 5 min, followed by incubation with the kit incubation buffer pH for 15 min at RT and incubation with 10 μ g/ml anti- β -tubulin in PBS for 1 hour at RT. Cells were then incubated with 50 μ l of anti-BrdU-FLUOS antibody combined with 1:200 donkey anti-mouse at 37°C for 1 hour and then rinsed 3 times in PBS at RT. Cover slips were mounted in PBS and sealed.

Immuno-fluorescence was evaluated by fluorescence microscopy using 1000× magnification.

2.2.10. Microscopy and imaging

Immunocytochemistry was visualized with appropriate fluorescence excitation filters for fluorescent microscopy (Olympus BX-50). Tiff format images of 30 random fields per cover slip were taken with a Pixera digital camera for microscopy at identical manual exposure setting for all experiments within each study. Fluorescence was measured by quantifying mean optical fluorescence of each image using Scion Image software with a 256 bit deep camera. The upper and lower 20 bits were cut off to eliminate non-specific fluorescence and a mean density of pixels/field within this range were obtained. The data were normalized for readings between 0 and 100 for statistical analysis, using the following formula:

$$[(\text{Pixels} \times \text{mean pixels}) / (\text{number of cells per random field of view})] / 10,000$$

2.2.11. Statistical analysis

All experiments were repeated 3-5 times using different preparations of adult mouse cortical neurons, microglia and reagents. The data in individual experiments were presented as mean \pm standard error and statistical analysis was performed using SPSS statistical software.

3. RESULTS

3.1. Characterization of adult mouse cortical culture

The three cell types in the AMC culture were identified by immunocytochemistry. The majority of the cell (approximately 70%) was neurons staining positive for β -tubulin (Fig. 1). Astroglia, staining with anti-GFAP and microglia staining with BSL1 were present in equal proportions, approximately 15% each (Fig. 1). These three markers identified an average of 97% of the viable cells present in a three-day old culture. Representative morphologies of immuno-stained cells are shown in Fig. 2. β -tubulin immuno-reactive cells displayed several long processes with branches. GFAP positive cells had shorter processes with many branches. Microglial cells were either branched or round, with numerous fine processes, known as cilia.

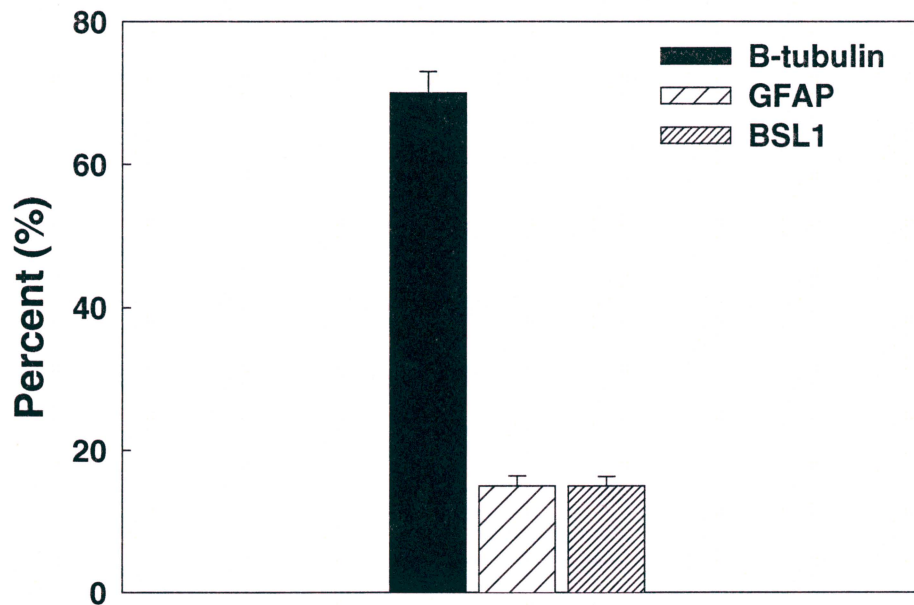


Figure 1. Immuno-fluorescent labeling of cell types in the adult mouse cortical culture. For each antigen, 6 cover slips were immuno-stained, and immuno-positive cell in 30 fields/slip were counted and expressed as a percentage of total viable cells. Values represent fraction of each cell type in AMC culture. Data are mean \pm S.E.M, $p < 0.05$.

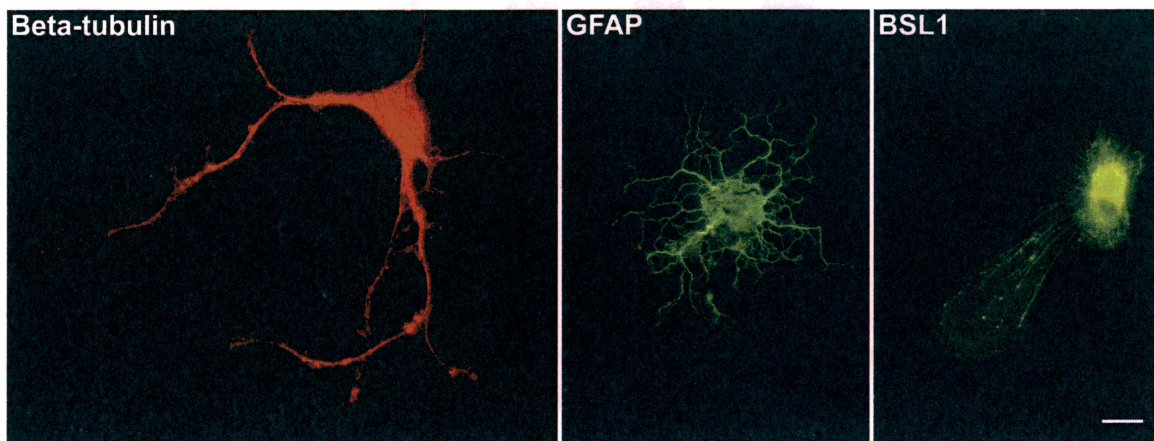


Figure 2. Representative morphologies of three cell types in AMC culture: neurons stained for β -tubulin, astrocytes stained for GFAP and microglia stained with BSL1. Fluorescent microscopy, 1000 \times magnification. Scale bar=10 μ m.

3.2. Accumulation of apoE3 and apoE4 in AMC neurons

The cell-associated apoE3 was significantly (Repeated Measures ANOVA, $F=2$, $df=78.738$, $p<0.01$) greater than apoE4 at all time courses at 37°C: at 5, 15, 30 and 60 minutes. At 4°C cell-associated apoE3 was significantly (Repeated Measures ANOVA, $F=2$, $df=1,78.738$, $p<0.01$) lower than apoE4 (Fig. 3,4). Immunoreactivity was primarily of a punctuate nature. Experiment was repeated 3 times with different cell cultures and reagents, 80 neurons were analyzed per treatment, per time course, per experiment.

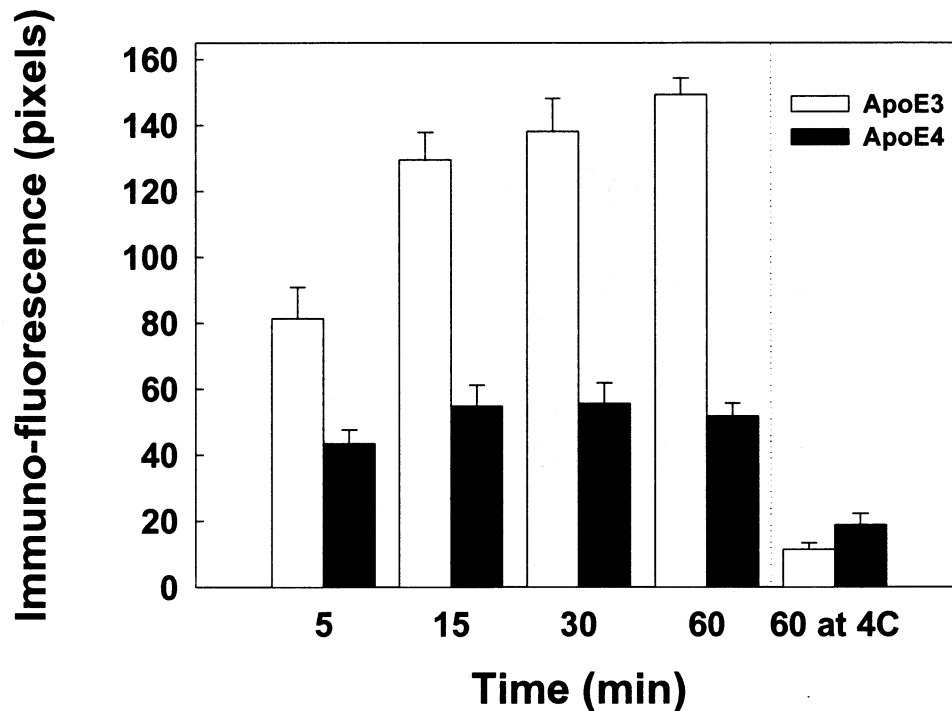


Figure 3. Quantification of accumulation of apoE3 and apoE4 in AMC neurons at 5, 15, 30 and 60 minutes at 37°C and at 60 minutes at 4°C. Values represent neuron-associated apoE3 and apoE4 at each time point and temperature, mean±S.E.M.

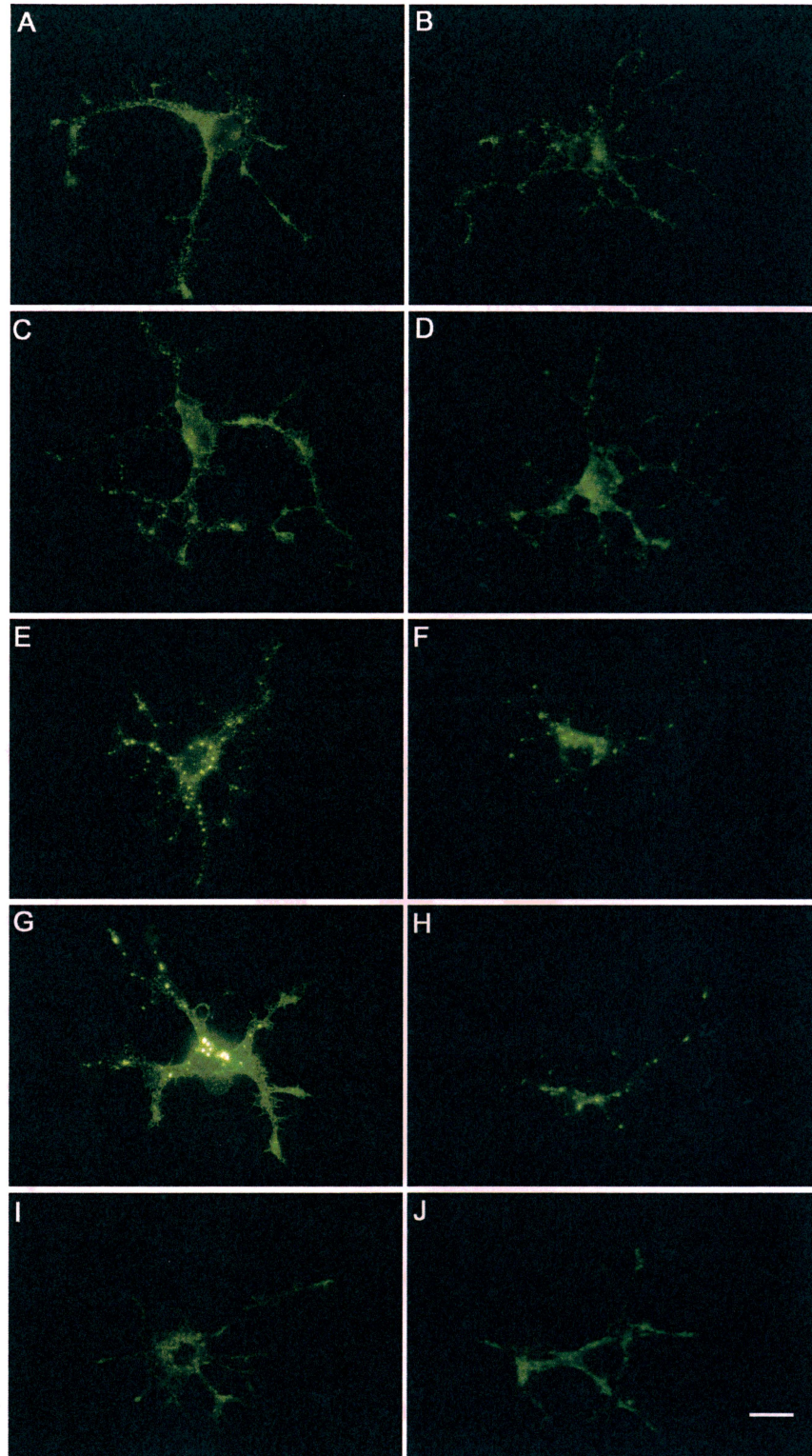


Figure 4. Accumulation of apoE3 and apoE4 in AMC neurons. *Left column:* apoE3. *Right column:* apoE4. *A-H:* incubation at 37°C. (A,B) apoE3 and apoE4 accumulation at 5 min. (C,D) at 15 min. (E,F) at 30 min. (G,H) at 60 min. (I,J) at 60 minutes at 4°C. Fluorescent microscopy, 1000× magnification. Scale bar=10 μm.

3.3. *Accumulation of apoE3 and apoE4 in somata and dendrites*

Analysis of immuno-fluorescence in apoE3 and apoE4 treatment groups at 5, 15, 30 and 60 minutes at 37°C and at 60 minutes at 4°C revealed that significantly (Repeated Measures ANOVA, $F=2$, $df=1,78.738$, $p<0.01$) more of apoE3 and apoE4 accumulated in somata than dendrites (Fig. 5,6). However, at all time points at 37°C, apoE3 level in dendrites was 30 or above, as measured in pixels of immuno-stain fluorescence, whereas accumulation of apoE4 in dendrites was below 10 pixels (Fig. 5,6).

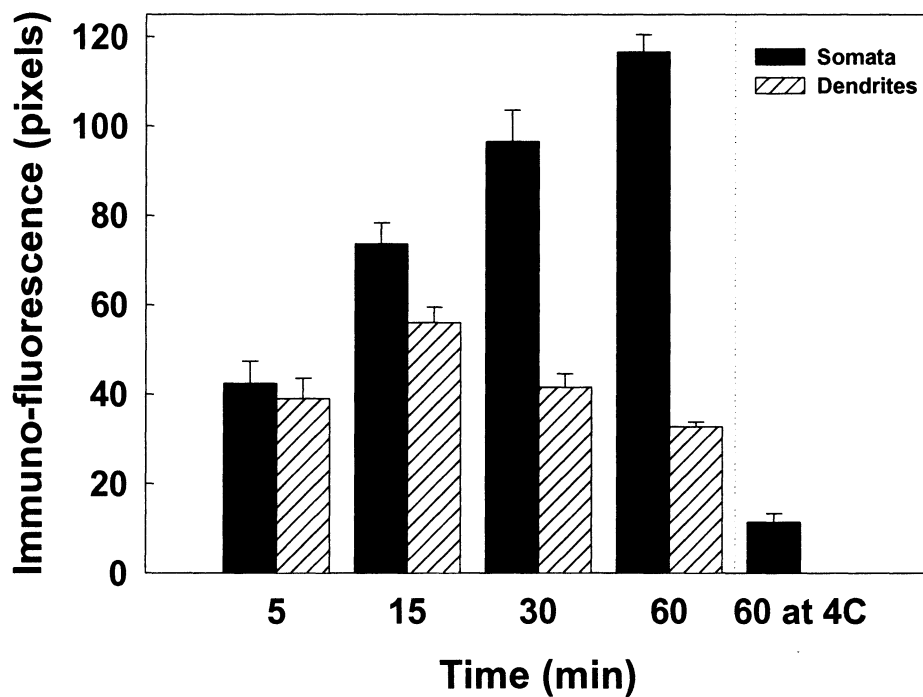


Figure 5. Quantification of accumulation of apoE3 in somata and dendrites in AMC neurons at 5, 15, 30 and 60 minutes at 37°C and at 60 minutes at 4°C. Values represent soma-associated and dendrite-associated apoE3 at each time point and temperature, mean±S.E.M.

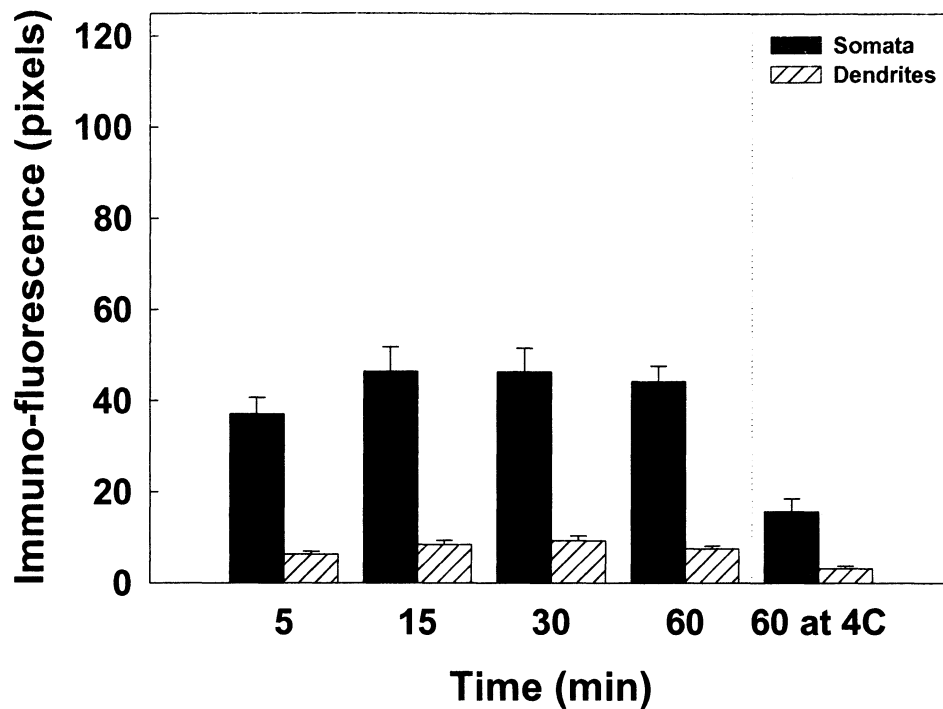


Figure 6. Quantification of accumulation of apoE4 in somata and dendrites in AMC neurons at 5, 15, 30 and 60 minutes at 37°C and at 60 minutes at 4°C. Values represent soma-associated and dendrite-associated apoE4 at each time point and temperature, mean±S.E.M.

Experiment was repeated 3 times with different cell cultures and reagents, 80 neurons were analyzed per treatment, per time course, per experiment.

3.4. Accumulation of apoE3 and apoE4 following inhibition of LRP-HSPG receptor complex

To test my hypothesis that apoE3 and apoE4 differential accumulation is mediated by LRP-HSPG receptor complex, I used LRP and HSPG inhibitors and analyzed apoE3 and apoE4 accumulation following the inhibition of LRP or HSPG. Pretreatment of apoE KO AMC neurons with known LRP receptor inhibitors RAP (5 µg/ml) and lactoferrin (10 µg/ml) [20] for 1 hour prior to incubation with apoE3 and apoE4 significantly

(MANOVA, $df=3,89$, $p<0.01$) decreased accumulation of apoE3 and apoE4, retaining the same significant difference in accumulation between apoE3 and apoE4 as was observed in the control group without LRP inhibitors (Fig. 7,8). Pretreatment of apoE KO AMC neurons with a known HSPG inhibitor heparinase I (10 units/ml) for 1 hour prior to incubation with apoE3 and apoE4 has shown that removal of HSPG completely abolished the difference between apoE3 and apoE4 and inhibited internalization of both apoE3 and apoE4 to undetectable amounts (Fig. 7,8). The experiment was repeated 3 times; images of 30 neurons were analyzed per apoE treatment, per inhibitor treatment, per experiment.

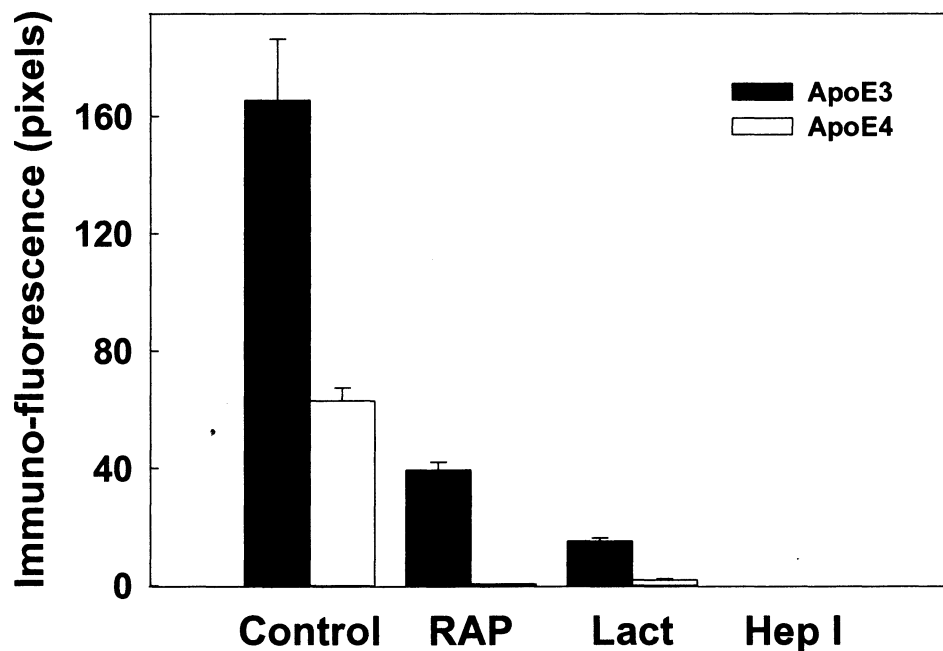


Figure 7. Quantification of accumulation of apoE3 and apoE4 in apoE KO AMC neurons at 1 hour, following the pretreatment of neurons with LRP receptor inhibitors RAP and lactoferrin, and with HSPG receptor inhibitor heparinase I. Values represent neuron-associated apoE3 and apoE4 for each inhibitor treatment, mean \pm S.E.M.

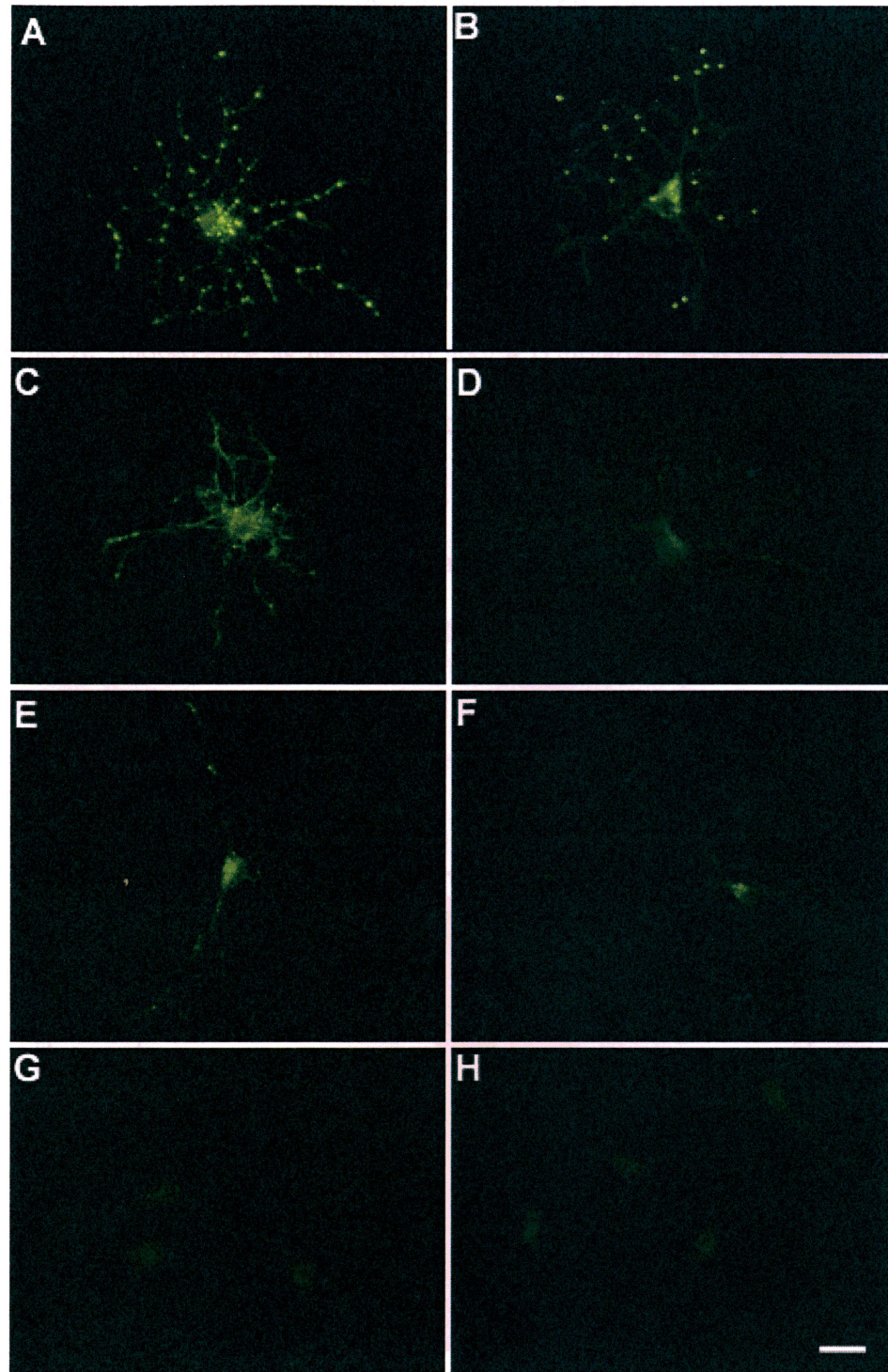


Figure 8. Accumulation of apoE3 and apoE4 in apoE KO AMC neurons at 1 hour, following the pretreatment of neurons with LRP-HSPG receptor complex inhibitors. *Left column: apoE3. Right column: apoE4. (A,B)* apoE3 and apoE4 accumulation in the absence of LRP-HSPG inhibitors. *(C,D)* apoE3 and apoE4 accumulation following pretreatment with RAP; *(E,F)* with lactoferrin; *(G,H)* with heparinase I. Fluorescent microscopy, 1000× magnification. Scale bar=10 μ m.

3.5. *Effect of apoE3 and apoE4 on fatty acid transport in AMC culture*

I predicted that apoE4 would deliver fewer lipids to neurons than apoE3 because the rate of uptake of apoE4 was slower than apoE3 in AMC neurons. To test this hypothesis, I examined fluorescently labeled dodecanoic acid accumulation in adult cortical neurons. AMC neurons cultured with apoE3 internalized approximately twice as much vesicular accumulations of fluorescence as those with apoE4 (Univariate ANOVA, Bonferroni t-test, $df=2,89$, $p<0.01$). Post hoc t-testing showed that $E3>E4>KO$ (no apoE) for total lipid uptake (Fig. 9). ApoE4 roughly doubled the amount of lipid internalized compared to the absence of apoE (Fig. 10). Therefore, although apoE4 was better than no apoE, it was much less effective than apoE3 in providing lipids. The experiment was repeated 3 times; the images of 30 neurons were analyzed per apoE treatment, per experiment.

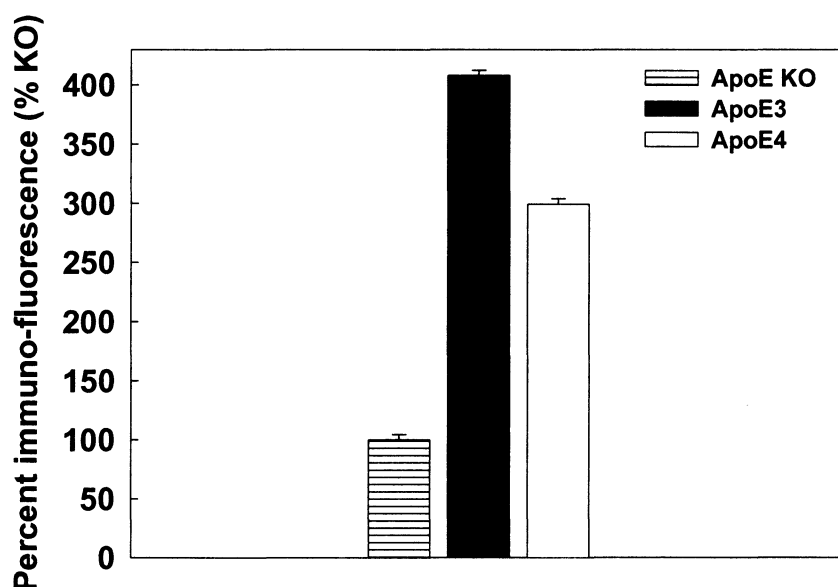


Figure 9. Percent of fluorescent fatty acid accumulation facilitated by apoE3 and apoE4 of fluorescent fatty acid accumulation in apoE KO AMC neurons at 1 hour after incubation. Values represent mean \pm S.E.M.

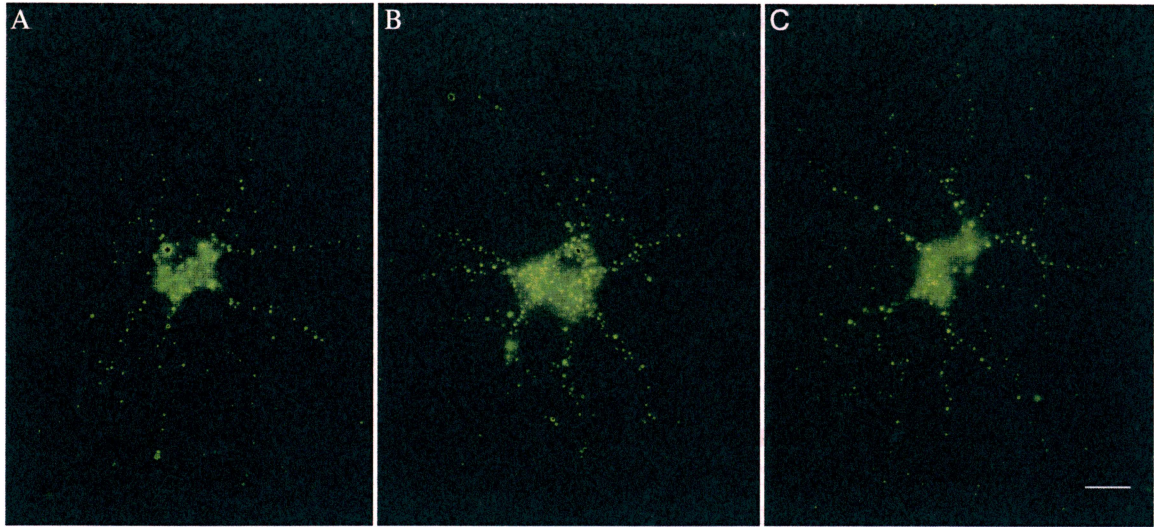


Figure 10. Fluorescence intensity of the fatty acid (BODIPY-FL) at 1 hour after incubation with apoE isoforms or in the absence of apoE (KO). (A) fatty acid accumulation without apoE; (B) fatty acid accumulation when co-incubated with apoE3; (C) with apoE4. Of note: apoE4 is better than no apoE. Fluorescent microscopy, 1000× magnification. Scale bar=10 μ m.

3.6. Effect of apoE3 and apoE4 on microglial proliferation and morphology in AMC culture

ApoE isoforms play an important role in both neuronal biology and neuronal environment. Based on previous studies on the differential effect of apoE3 and apoE4 peptides on microglial number and morphology and activation [14, 21] in embryonic and postnatal neuronal cultures, I proposed and tested the hypothesis that apoE3 and apoE4 differentially regulate microglial number, morphology and activation in AMC culture. I compared effects of human apoE3 and apoE4 on microglial number in apoE KO AMC cultures. AMC cultures treated with human apoE4 had significantly (Univariate ANOVA, Bonferroni t-test, $df=2,89$, $p<0.01$) higher number of microglia per field than apoE3 treatments, in total of 90 fields per treatment analyzed (Fig. 11). The highest microglial

number per field was observed in the absence of apoE (KO) (Fig. 11). ApoE KO cultures had on average approximately 13 microglia per 200 μm^2 , whereas apoE4 treatment group had on average 11 microglia per 200 μm^2 and apoE3 treatment group had only 9 microglia (Fig. 11).

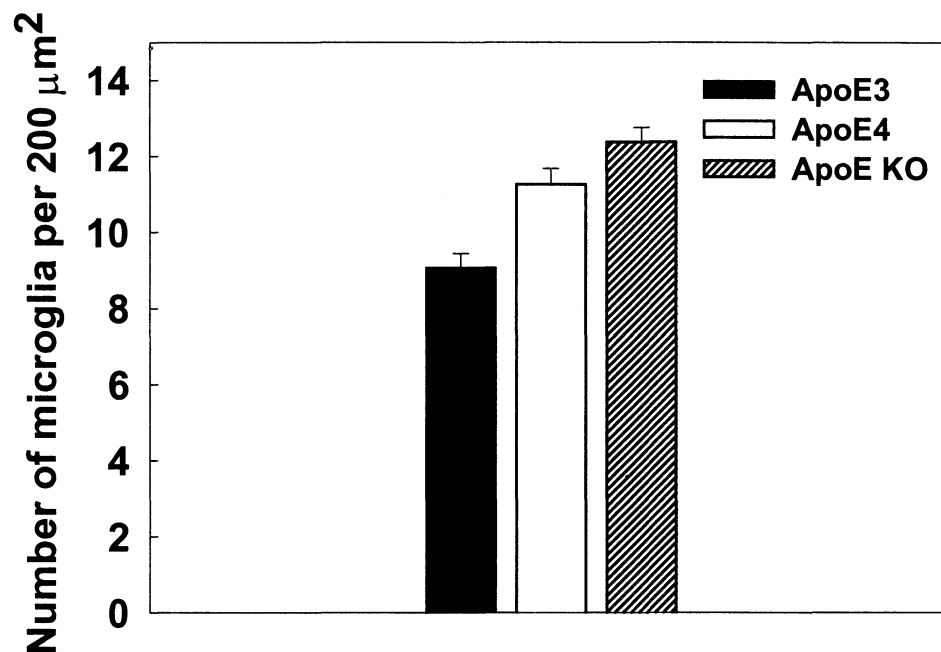


Figure 11. Effect of human apoE3, apoE4 and absence of apoE (KO) on microglial proliferation in apoE KO AMC culture. Values represent mean \pm S.E.M.

As previous studies have shown, microglia respond to damage or infection by proliferation and changing the morphology to macrophage-like phagocytic cells [15]. In all three apoE treatment groups significant (Univariate ANOVA, Bonferroni t-test, $df=2,89$, $p<0.01$) impact on microglial morphology was observed. ApoE KO and apoE4 groups were represented by 76% and 50% macrophage-like microglia, respectively,

whereas apoE3 group had only 20% of macrophage-like microglia (Fig. 12, 13). The experiment was repeated 3 times, morphology of microglia in 30 fields (10 fields per cover slip) were analyzed per apoE treatment, per experiment.

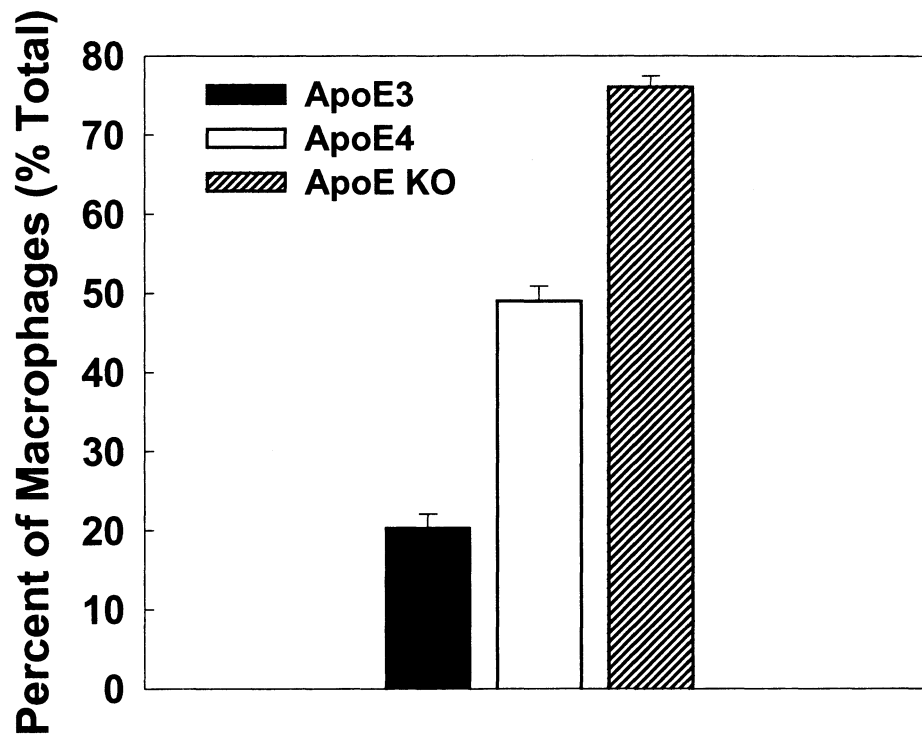


Figure 12. Effect of human apoE3, apoE4 and absence of apoE (KO) on microglial morphology in apoE KO AMC culture. Values represent percent of macrophage microglia in each treatment group, mean \pm S.E.M.

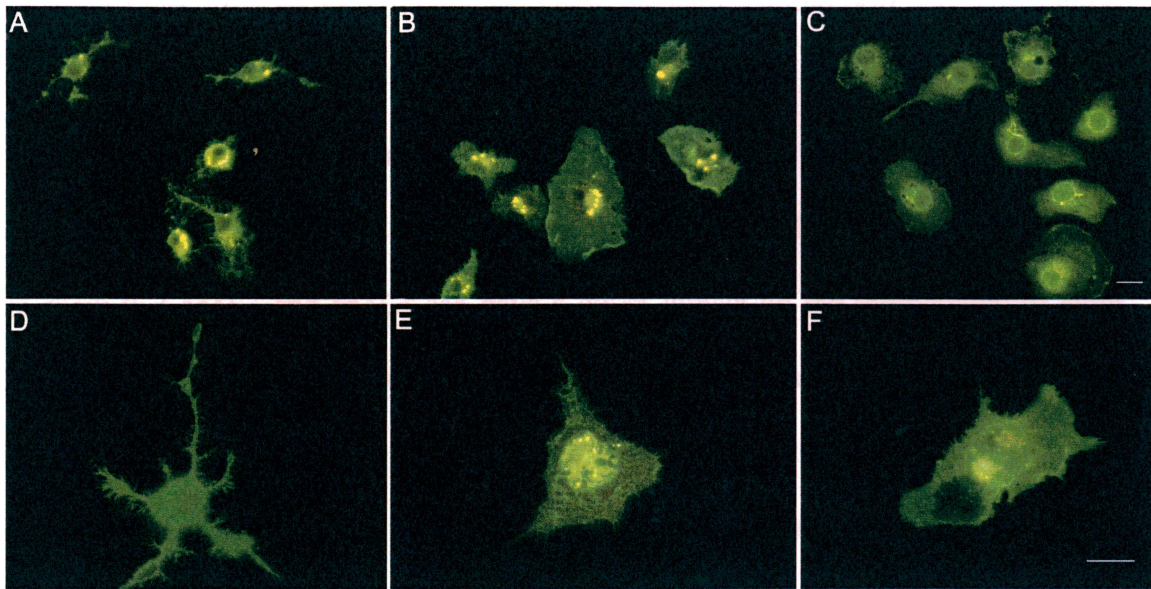


Fig. 13. Effect of apoE isoforms and absence of apoE on microglial morphology in adult mouse cortical culture. *Top row:* immuno-positive cells under 60× objective. (A), AMC culture microglia incubated with apoE3 have structured ciliated morphology. (B), AMC culture microglia incubated with apoE4 have macrophage morphology. (C), apoE KO AMC culture microglia are predominantly macrophage-like. Scale bar=10 μ m. *Bottom row:* immuno-positive cells under 100× objective. (D), representative morphology of AMC culture microglia when treated with apoE3, (E), representative morphology of AMC culture microglia when treated with apoE4, (F), morphology of AMC culture microglia in the absence of apoE. Scale bar=10 μ m.

3.7. Effect of apoE3 and apoE4 on microglial proliferation and morphology in adult mouse microglial (AMM) culture

To determine whether human apoE3 and apoE4 have a direct effect on adult mouse microglial number and morphology in the absence of neurons and astrocytes, I prepared pure microglial (99.5%) adult mouse cultures as described in Methods. Like AMC cultures, microglial cultures were treated with 3 μ g/ml of human apoE3 and apoE4 at 2 and 3 DIV, and then fixed on day 4 to assess the cell proliferation and morphology. In

apoE4 treatment group microglial number was significantly (Univariate ANOVA, Bonferroni t-test, $df=2,89$, $p<0.01$) higher than in the apoE3 group (Fig. 14). The highest number of cells per field was observed in the apoE KO group (Fig. 14). The pattern of cell proliferation due to apoE isoforms treatments in AMM cultures was very similar to microglial proliferation in AMC cultures treated with apoE3 and apoE4 (Fig. 11, 14). The data show that apoE3 and apoE4 can have a direct impact on the morphology of adult microglia and that treatments with apoE4 result in a higher number of adult microglia with predominant macrophage morphology. The experiment was repeated 3 times, morphology of microglia in 30 fields (10 fields per cover slip) were analyzed per apoE treatment, per experiment.

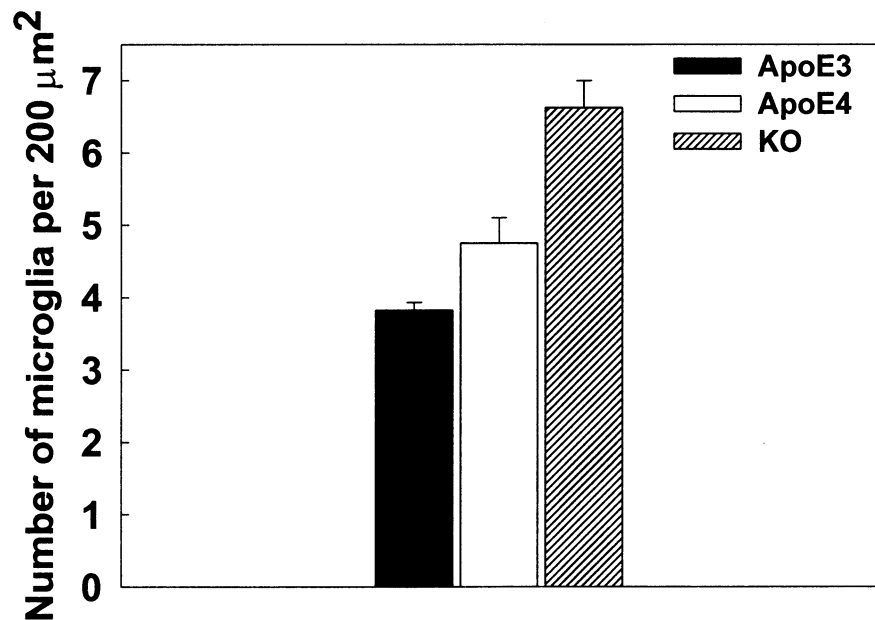


Figure 14. Effect of human apoE3, apoE4 and absence of apoE (KO) on microglial proliferation in apoE KO AMM culture. Values represent mean \pm S.E.M.

Morphological study of AMM cultures showed that apoE isoforms have a significantly (Univariate ANOVA, Bonferroni t-test, $df=2,89$, $p<0.01$) different effect on microglia in the absence of neuron-microglia and astocyte-microglia interactions, and that this effects is similar to the one observed in AMC culture. ApoE KO group had the highest percentage (76%) of macrophage microglia, followed by apoE4 group at 58% and apoE3 group at 34% (Fig. 15, 16). These data show that apoE4 and the absence of apoE up-regulate cell number in AMM cultures, just as they do in AMC cultures.

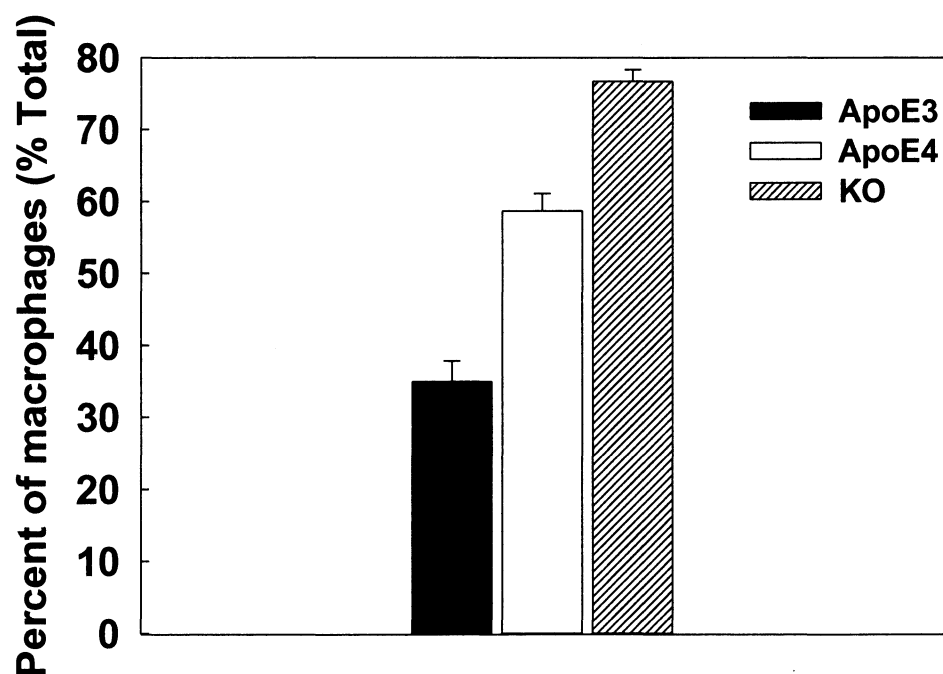


Figure 15. Effect of human apoE3, apoE4 and absence of apoE (KO) on microglial morphology in apoE KO AMM culture. Values represent percent of microphage microglia in each treatment, mean \pm S.E.M.

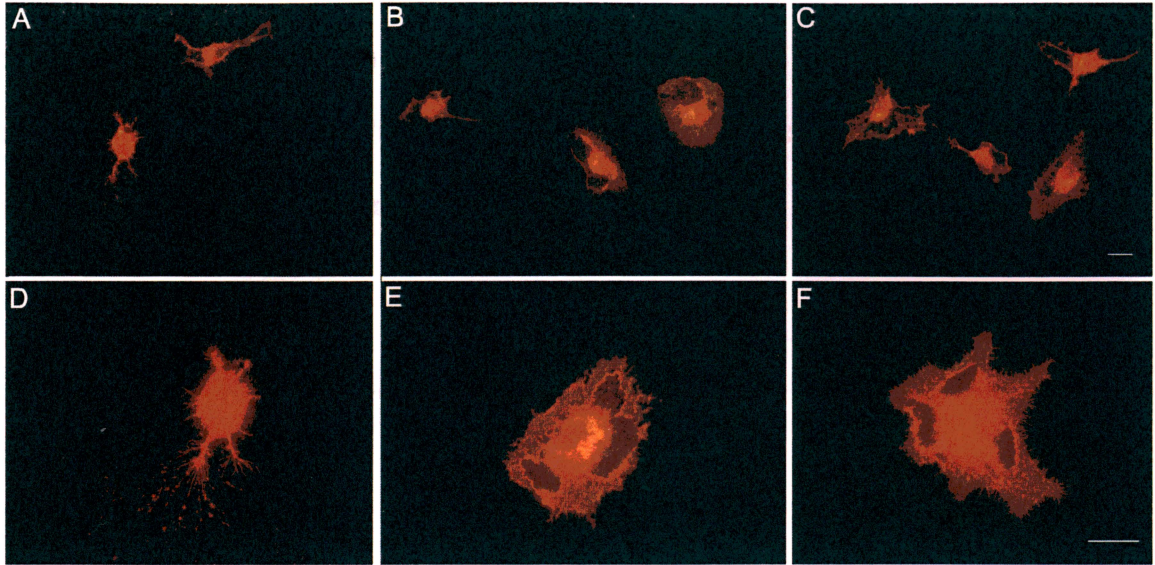


Figure 16. Effect of apoE isoforms and absence of apoE on morphology in adult mouse microglial culture. *Top row:* immuno-positive cells under 60× objective; (A) AMM culture incubated with apoE, (B) AMM culture incubated with apoE4, (C) apoE KO AMM culture. Scale bar=10 μm. *Bottom row:* immuno-positive cells under 100× objective. (D, Representative morphology of AMM culture microglia treated with apoE3, (E) Representative morphology of AMM culture microglia treated with apoE4, (F) in the absence of apoE (apoE KO). Scale bar=10 μm.

3.8. Effect of apoE3 and apoE4 on iNOS production in AMC culture

To determine whether predominant macrophage morphology of microglia in apoE4 and apoE KO groups is correlated with microglial activation, I measured the inducible nitric oxide synthase (iNOS) production by microglia in AMC culture. LPS, a classic neuroinflammatory stimulus was added 12 hours before fixing. I examined iNOS levels in apoE3, apoE4 and no apoE treated AMC culture cell medium at 4 DIV by immunoblotting as described in Methods. A significantly (Univariate ANOVA, Bonferroni t-test, $df=2,2$, $p<0.02$) elevated level of iNOS was detected in apoE KO AMC culture cell

medium (Fig. 17, 18). These data indicate that the absence of apoE results in the highest level of microglial activation in AMC culture when compared to apoE3 and apoE4. Presence of apoE4 resulted in significantly higher microglial activation than of apoE3 treatment in AMC cultures (Fig. 17, 18). Cell medium was collected from 3 wells per apoE treatment, per experiment.

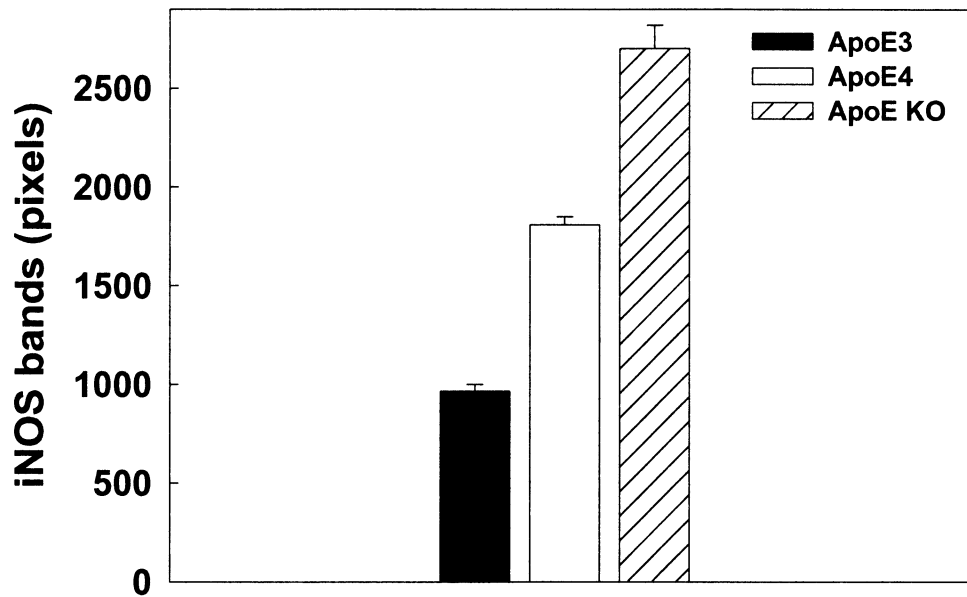


Figure 17. Quantification of iNOS levels in apoE3, apoE4 treated AMC culture and apoE KO culture by Western Blotting. Values represent mean \pm S.E.M.

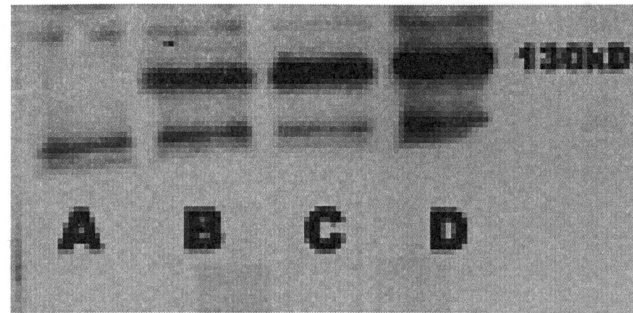


Figure 18. Effect of apoE3, apoE4 and absence of apoE (KO) on iNOS production by AMC culture microglia: (A) growth medium without cells, (B) medium from apoE3 treated cells, (C) apoE4 treated cells, (D) apoE KO cells.

3.9. Effect of apoE3 and apoE4 on neurogenesis in AMC cultures

Based on the previous findings on neurogenesis in adult brain [16] and my observations of neurogenesis in AMC cultures, I proposed that apoE3 and apoE4 might have differential effect on neurogenesis in AMC culture. To test this hypothesis, AMC cultures were treated with human apoE3 and apoE4 at 2 and 3 DIV. At 4 DIV total cell proliferation was assessed by MTT cell proliferation kit and ELISA. No significant (Univariate ANOVA, Bonferroni t-test, $df=2,11$, $p>0.05$) difference in cell number between apoE3, apoE4 and no apoE (KO) treatments was detected (Fig. 19). The experiment was repeated 3 times, absorbance values from 12 wells per apoE treatment, per experiment (using 96-well microtiter plates) were analyzed and compared. The count

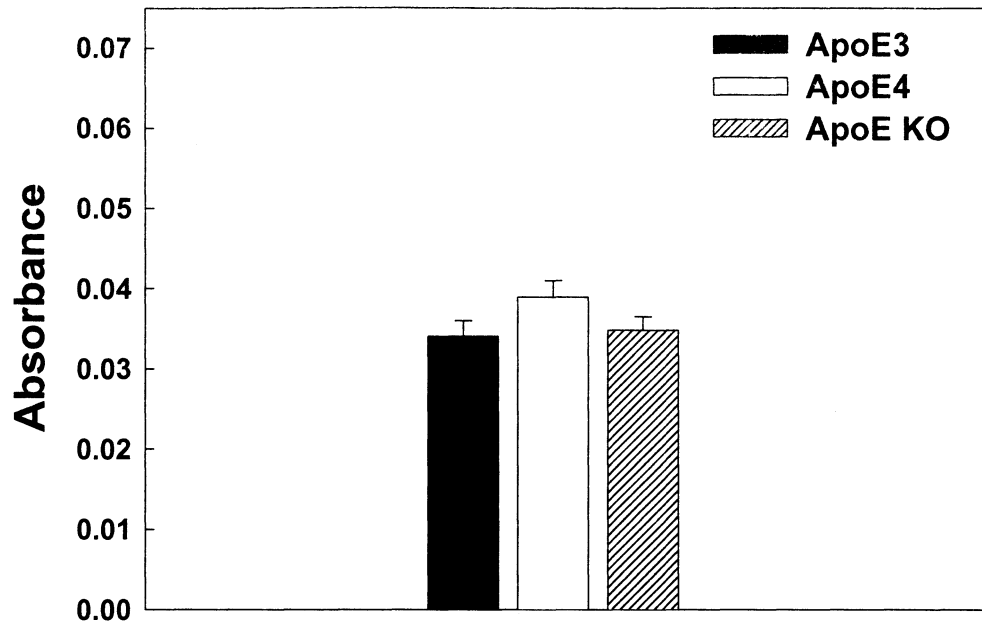


Figure 19. Effect of apoE3, apoE4 and absence of apoE (apoE KO) on cell proliferation in AMC culture at 4 DIV. Values represent mean±S.E.M.

Since AMC culture is represented by three cell types (Results 3.1.) and microglial proliferation is higher in apoE4 and apoE KO than in apoE3 treated cells by 4 DIV (Results 3.6.), my next aim was to determine the number of neurons by neuron specific β -tubulin immunocytochemistry in apoE3, apoE4 and apoE KO AMC cultures and compare the number of neurons between these treatments at 4 DIV. AMC cultures were treated with 3 μ g/ml of human apoE3 and apoE4 at 2 and 3 DIV. At 4 DIV cells were fixed, immuno-stained for β -tubulin and counted in 30 random fields per cover slip. The count showed E3>E4>KO for average number of neurons per field, but no significant (Univariate ANOVA, Bonferroni t-test, $df=2,89$, $p>0.05$) difference in the number of neurons between apoE3, apoE4 and no apoE (KO) treatments was detected by Post Hoc

testing (Fig. 20). The experiment was repeated 3 times, 30 fields (10 fields per cover slip) were analyzed per apoE treatment, per experiment.

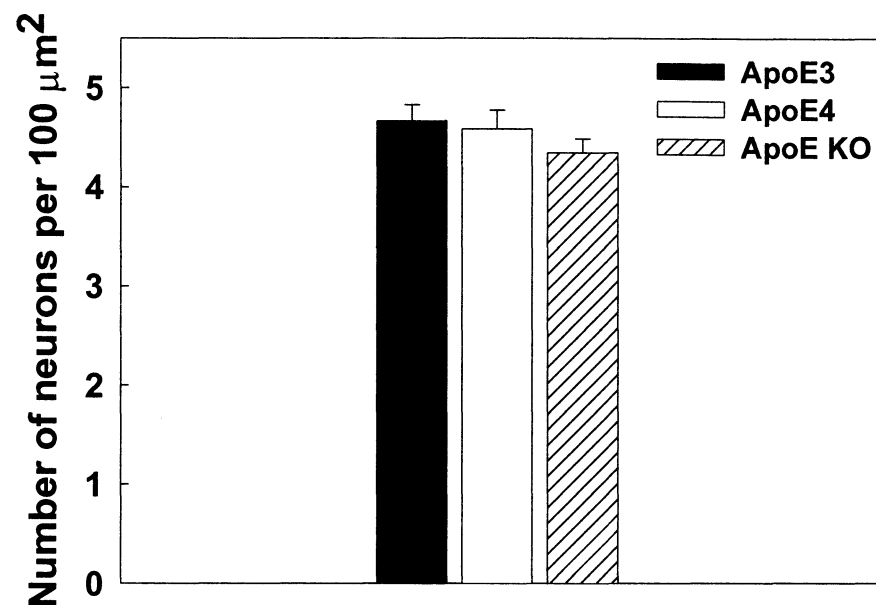


Figure 20. Effect of apoE3, apoE4 and absence of apoE (apoE KO) on proliferation of neurons in AMC culture at 4 DIV. Values represent mean±S.E.M.

To determine if a slight but not significant difference in neuron number in AMC culture at 4 DIV in apoE3, apoE4 and apoE KO treatments accounts for neurogenesis, I treated apoE KO AMC cultures with 3 μg/ml of human apoE3 and apoE4 at 2 and 3 DIV, fixed cells and performed double immunocytochemistry for β-tubulin and BrdU. Since it has been shown that 5-bromo-2'-deoxyuridine (BrdU), a thymidine analogue, shares S phase labeling characteristics with [3H]-thymidine, immunochemical detection of BrdU incorporation into DNA has become a powerful tool for identifying cells in which DNA synthesis has occurred. In apoE3, apoE4 and apoE KO treatments BrdU stain was picked

up by many non-neuronal cells (Fig. 21, A) determined by their non-specificity to β -tubulin (Fig. 21,B).

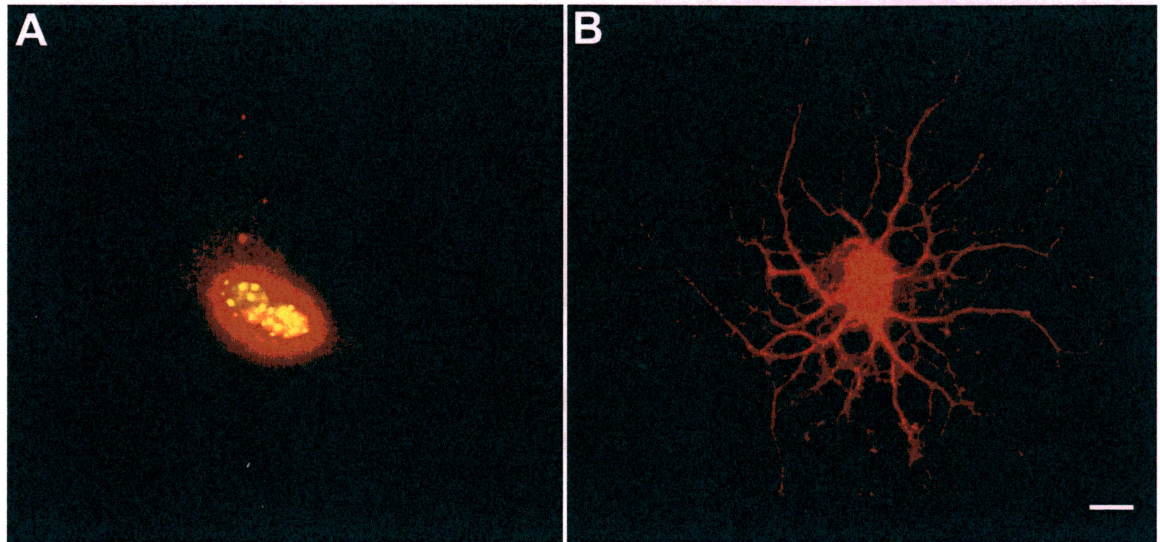


Figure 21. (A) BrdU-positive cell of non-neuronal origin in AMC culture at 4 DIV. (B) BrdU-negative neuron in AMC culture at 4 DIV. Fluorescent microscopy, 1000 \times magnification. Scale bar=10 μ m.

However, a number of BrdU-positive neurons were detected in apoE3, apoE4 and apoE KO treatment groups (Fig. 22).

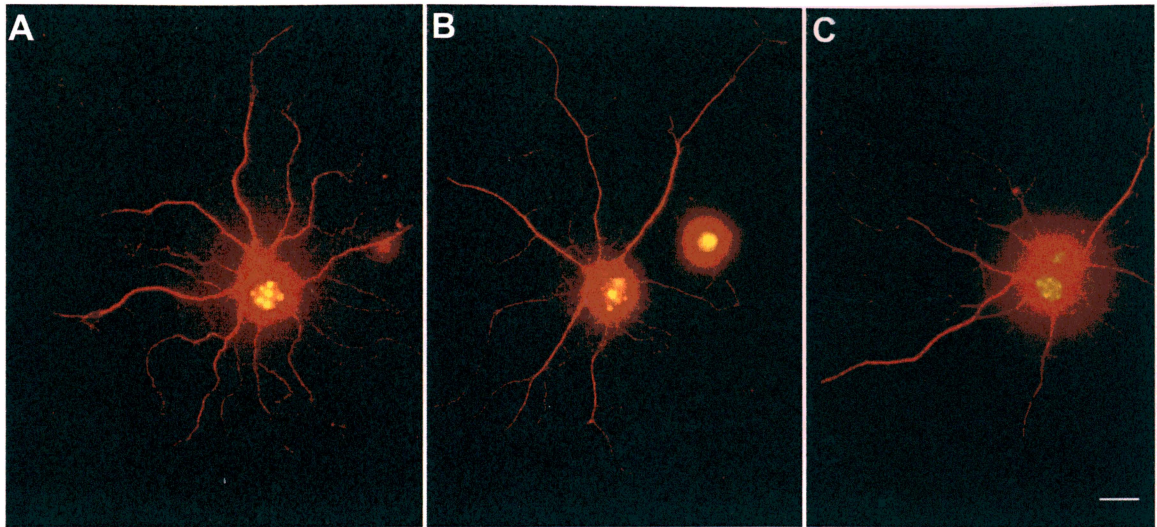


Figure 22. BrdU-positive neurons in AMC culture at 4 DIV treated with (A) apoE3; (B) apoE4; (C) no apoE (KO). Fluorescent microscopy, 1000 \times magnification. Scale bar=10 μ m.

A significantly (Univariate ANOVA, Bonferroni t-test, $df=2,89$, $*p<0.01$) higher number of BrdU-positive neurons were detected in apoE3 treatment group than in apoE4 or apoE KO (Fig. 23). Post Hoc testing showed no significant (Univariate ANOVA, Bonferroni t-test, $df=2,89$, $**p>0.05$) difference between the number of BrdU-positive neurons in apoE4 and apoE KO (Fig. 23). The experiment was repeated 3 times, 30 fields (10 fields per cover slip) were analyzed per apoE treatment, per experiment.

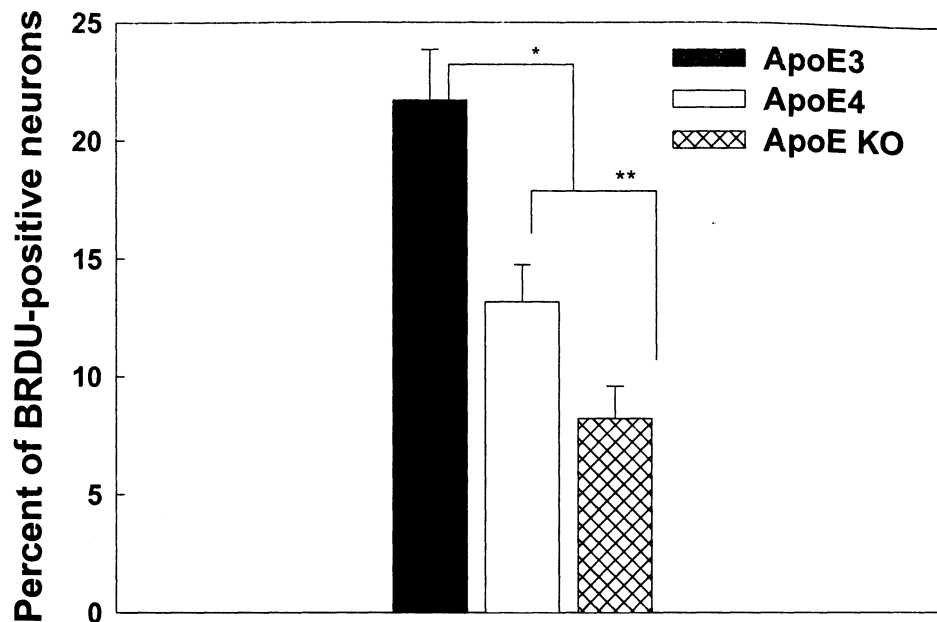


Figure 23. Effect on apoE3, apoE4 and no apoE (apoE KO) on neurogenesis in AMC culture at 4 DIV. Values represent mean±S.E.M.

3.10. BrdU-positive satellite stain phenomenon in BrdU-positive neurons

In approximately 50% of BrdU-positive neurons in apoE3, apoE4 and apoE KO treatment groups a BrdU-positive satellite staining was detected. This staining did not correspond to debris of stain clusters. It appeared to correspond to a cell body of undifferentiated cell and was located in a dendritic tree or at a terminal bouton or at perikaryon of a neuron. Fluorescent and bright field microscopy with 100× objective shows the satellite cell body and incorporation of BrdU stain in a satellite cell (Fig. 24). BrdU-positive satellite cells were detected in all three experiments (Results 3.10); 30 fields (10 fields per cover slip) were analyzed per apoE treatment, per experiment.

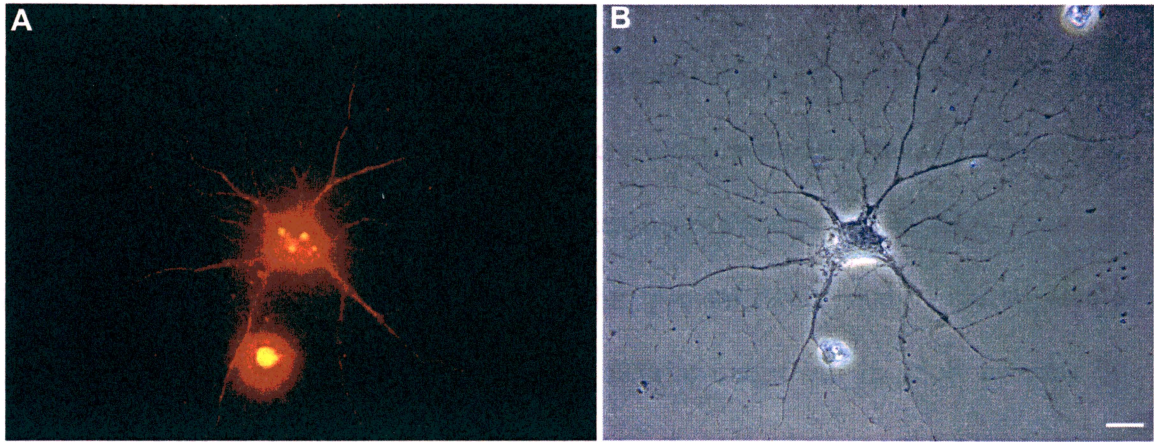


Figure 24. Image of BrdU-positive AMC neuron at 4 DIV with BrdU-positive satellite stain along a dendrite taken with (A) Fluorescent filter, 100× objective; (B) Bright field microscopy, 100× objective. Scale bar=10 μ m.

4. DISCUSSION

Important previous research on the differential effect of apoE3 and apoE4 on neurite outgrowth of adult neurons [5] suggested a mechanism by which apoE may lead to AD. That study showed that apoE3 increases neurite outgrowth in AMC neurons, whereas apoE4 inhibits neurite outgrowth. In the present recent study I investigated a possible mechanism by which apoE4 inhibits neurite outgrowth in adult neurons by comparison of (1) apoE3 and apoE4 accumulation rate in the neurons and (2) in somata and dendrites, (3) apoE3 and apoE4 binding rate to apoE receptor complex on neuronal membrane surface and (4) apoE3 and apoE4 rate of lipid transport. I also investigated (6) the roles of apoE3 and apoE4 on neuronal proliferation (neurogenesis) and (5) their roles on neuronal environment – microglia.

Results of my studies show (1) apoE3 and apoE4 differentially accumulate in AMC neurons; (2) differential binding of apoE3 and apoE4 in AMC neurons is mediated by HSPG receptor of LRP-HSPG receptor complex; (3) apoE3 and apoE4 differentially transport lipid to AMC neurons; (4) apoE3 and apoE4 have a differential effect on microglial number, morphology and activation in both AMC and AMM cultures and (5) apoE3 and apoE4 have a differential effect on neurogenesis in AMC cultures. Furthermore, results of the experiment dealing with effect of apoE3 and apoE4 on neurogenesis in AMC neurons reveal a new feature of cortical neurogenesis – BrdU-positive satellite cells in the dendritic tree of approximately half of the studied adult neurons in DNA synthesis phase.

(1) The results of the study on the isoform-specific cellular accumulation rate of apoE over a time course of 1 hour in AMC neurons is consistent with the results of a

previous study on the differential accumulation rate of apoE3 and apoE4 in Neuro-2a neuroblastoma cell line. [22]. However, results of the present study reveal two new significant features when compared to the study of apoE isoforms in neuroblastoma cell line: (1) differential cell biology of apoE isoforms in adult brain model and (2) the pattern of distribution of apoE isoforms in somata and dendrites of adult neurons.

The plasticity and functionality of the network of neurites in the adult brain depends on the strength, health and branching of neurites and their capability to grow and repair. Neurites, a term that cumulatively describes dendrites and an axon of a neuron, are extensions of neuronal membrane, comprised of a thin double layer of fatty acids - one of many molecules that are long chains of lipid-carboxylic acid found in fats and oils and in cell membranes, as a component of phospholipids and glycolipids. The growth and regeneration of the neurites depends on the supply of fatty acids and lipids to the neurons [23, 24], where apoE plays a vital role as a transport lipoprotein that ensures the supply.

(2) Results of my study showed that apoE4 accumulated significantly slower in AMC neurons than apoE3. Moreover, less apoE4 accumulates specifically in neurites than apoE3. These data suggest that neurons that function in a system where apoE4 is present do not have an adequate amount of lipid transporter reaching their neurites.

(3) The site where the difference in apoE3 and apoE4 binding takes place was also determined. When HSPG receptor of LRP-HSPG receptor complex was removed no binding or accumulation of either apoE3 and apoE4 occurred, which indicates that HSPG plays a pivotal role in apoE isoforms uptake. Previous study [25] suggests that HSPG is a 'helper' receptor in the LRP-HSPG receptor complex, a ligand that allows LRP to

internalize apoE isoforms, and that HSPG as a receptor by itself is less efficient than LRP.

The results of my study show that inhibition of LRP significantly decreases apoE3 and apoE4 uptake, but does not abolish the difference in their uptake. This data suggests that when the LRP receptor is blocked, the HSPG 'helper' receptor differentially mediates apoE isoform uptake and at a lower rate, as previous study suggested [25]. The differential binding of apoE3 and apoE4 to HSPG binding domain, rich with SO₄ groups [26], may be due to differential amino acids at the position 112 in receptor binding domain of apoE3 (cysteine) and apoE4 (arginine). The further study of cystein-SO₄ groups and arginine-SO₄ groups interactions may explain the basis for differential binding of apoE3 and apoE4 to HSPG.

Differential accumulation rates of apoE3 and apoE4 shown in my study suggest that the shortage of apoE, associated with apoE4, in neurons may be the basis of inhibited neurite outgrowth in apoE neurons. Furthermore, lower concentrations of cellular apoE4 within the neurites may explain the stunted neurite outgrowth. The binding pattern at 5 minutes of incubation with apoE isoforms indicated that apoE receptors were distributed through out the whole cell surface of neurites. The internalization pattern showed that apoE isoforms movement inside the cell is directed toward somata with dense accumulation of apoE vesicles in the somata after 60 minutes of incubation at 37°C. However when comparing two isoforms, apoE4 was present at a much lower concentration along the dendrites. Interestingly, significantly more apoE4 was bound to neuronal surface than apoE3 after 60 minutes at 4°C, but no intracellular accumulation occurred at this low temperature.

What is the impact of shorter neurites in neuronal health and performance? The shorter neurite outgrowth in apoE4 transgenic mice may be a cause of poorer neuronal plasticity [27], performance [28] and regeneration after injury in apoE4 individuals [29], as previous studies have shown. Based on the data of my study, I suggest that the primary cause of shorter neurite outgrowth and consequently poorer neuronal circuitry and ability to regenerate, associated with apoE4, may be a lesser amount of the lipid transporter, apoE4, in adult neurons.

(4) However, the more important evidence for shorter neurite outgrowth in apoE4 neurons would be a smaller amount of fatty acid, a building block of neuronal membrane, delivered to the neuron by apoE4. About two-thirds of brain is composed of fats. Fatty acids, the simplest lipids, are just as important as vitamins and minerals, but unlike these micronutrients that are required only in tiny amounts, fatty acids are needed in relatively large quantities. Previous study has shown that incubation of β -VLDL (very low density lipoprotein) with apoE3 resulted in increased neurite outgrowth when compared with incubation of β -VLDL with apoE4 [22].

I predicted that apoE4 would deliver fewer lipids to neurons than apoE3 because the rate of uptake of apoE4 was slower than apoE3 in neurons. Investigation of fluorescently labeled dodecanoic acid accumulation in live adult cortical neurons, facilitated by apoE3, apoE4 or no apoE (KO) revealed that apoE3 delivers substantially more fatty acid to neurons than apoE4. The smallest amount of fatty acid accumulated in neurons in the absence of apoE (apoE KO), pointing to the previously established role of apoE as a lipid transport protein [3]. Fluorescently labeled dodecanoic acid was used as a lipid probe. It is a fluorescent fatty acid analog that has been used for lipid trafficking

studies and as a general membrane probe. This analog has been tested before in several studies and shown to undergo native-like transport and metabolism in cells [30]. Cells cultured with apoE3 internalized approximately twice as much vesicular accumulations of fluorescence as those with apoE4. ApoE4 roughly doubled the amount of lipid internalized compared to the absence of apoE (apoE KO). Therefore, although apoE4 was better than no apoE, it was much less effective than apoE3 in providing lipids. This data suggests that smaller amounts of lipid associated with slower internalization of the lipid transporter apoE4 may be a cause of shorter neurite outgrowth in adult neurons.

I propose the following model for the role of apoE4 in poor neuronal growth, repair and regeneration possibly associated with development of AD: slower binding of apoE4 results in fewer apoE4 in adult neurons and especially neurites; fewer apoE4 delivers fewer fatty acid required for neurite growth and repair, thus resulting in shorter neurite outgrowth.

Preparation of adult culture strips cells of all processes. During the next three days extensive neurite outgrowth occurs. Functional apoE supplies lipids for membrane formation. In the absence of functional apoE, neuronal membrane formation is slowed. Future studies on the agents that may increase apoE4 uptake and bring it to the level of apoE3 may help improve neuronal growth and regeneration associated with apoE4.

(5) My next study shows that apoE isoforms also have differential effect on neuronal environment - microglia. Microglial cells derive from hematopoietic stem cells, share many properties with tissue macrophages and have important functions in neuronal-glial network. In the normal brain, microglia is in a non-activated state and has branched ciliated morphology. Microglia respond to damage or infection by proliferation and

changing the morphology to macrophage-like phagocytic cells, which produce immune response.

My study demonstrates that apoE regulates microglial proliferation and activation in adult mouse cortical and adult mouse microglial cultures. Absence of apoE up-regulated microglial activation and number in adult mouse models used in these experiments. ApoE KO adult mouse cortical and microglial cultures had the highest number of activated microglia and the highest iNOS level. ApoE4 treated cultures also had numerous activated microglia and a higher level of iNOS. Only apoE3 treated cultures had lower number of activated microglia and lower level of iNOS. ApoE3 treated adult cultures were represented by a large fraction of ciliated, process-bearing non-activated microglia. Moreover, these data show that the differential effect of apoE isoforms on microglial proliferation and activation is not facilitated by neuron-microglia interactions, but is a result of direct effect of apoE on microglial biology.

These results are consistent with previous studies that show mice expressing apoE4 isoform have a greater NO production than mice expressing the apoE3 isoform [21, 31].

NO is generated following activation of NOS. There are three known NOS isoforms: neuronal NOS (nNOS), endothelial NOS (eNOS), and inducible NOS (iNOS). iNOS is not expressed in healthy tissue, but can be induced following various pathologic insults including viral infection [32]. Previous study show that (1) nitric oxide associated with elevated levels of iNOS had a neurodegenerative effect on rat substantia nigra dopaminergic neurons, following LPS induction and (2) LPS-induced loss of dopaminergic neurons was significantly inhibited by the administration of a selective inhibitor of iNOS [33]. A study of the NO effects on differentiated neuroblastoma cell

line Neuro2a, show that cell death and neurite retraction were partly reduced when NO production was inhibited by nitric oxide synthase inhibitors; the study suggest that inflammatory processes, which are partly transmitted via NO metabolites, may affect neurite extension and thus may contribute to degenerative changes in Alzheimer's disease [34].

Previous study on iNOS have also shown that, once translated, iNOS is functionally active and produces NO for sustained periods of time and that neuronal death following iNOS activation occurs slowly over time with the morphologic features of apoptosis [32].

My present study shows that after 2 days of treatment, physiological levels (3 $\mu\text{g/ml}$) of apoE4 up-regulated iNOS production nearly 2-fold in comparison to iNOS levels in apoE3 treated adult cortical cultures, suggesting that inheritance of e4 allele may be a risk factor for NO associated neurotoxicity in such individuals.

Results of previous studies show (1) a significant increase in amyloid plaques in the AD patients with allele e4 of apoE and (2) that senile plaques in the AD patients are surrounded by activated microglia and reactive astrocytes [11, 12, 13]. It has also been reported that inflammatory responses by cytokines and oxygen free radicals such as nitric oxide (NO) are associated with amyloid deposits in AD brains. A recent study investigated regional expression of iNOS and nNOS in the brains of patients with dementia with Lewy bodies (DLB) compared with those of patients with AD and non-demented elderly persons. In that study, overexpression of iNOS was demonstrated in the amygdala, hippocampus, entorhinal and insular cortices of DLB brains, the most vulnerable regions in DLB brains, as well as AD brains [35]. Glial

involvement was also found around neuritic plaques and extracellular neurofibrillary tangles [35].

Based on these recent findings and my present study, one would expect to find all of the following in the AD brain of individuals with e4 allele: (1) amyloid plaques, (2) extracellular neurofibrillary tangles, (3) smaller neurite extension, (4) elevated number of activated microglia, surrounding plaques and tangles and (5) elevated levels of iNOS and NO. However, the question now arises: are numerous activated microglia and elevated iNOS and NO levels a consequence or a possible cause of neuropathology found in AD brain?

Since three of the above mentioned hallmarks of apoE4-associated AD pathology could be found in a healthy adult brain of an individual with e4 allele, I suggest that one of the major AD risk factors could be the constant elevated number of activated microglia and iNOS levels, which over years may have accumulated neurodegenerative effect and lead to AD pathology.

Previous studies show that iNOS and NO levels are elevated even in the non-aged adult animal transgenic models with e4 allele, before senile plaques and neurofibrillary tangles could be detected in their brains [21]. My present study shows that physiological levels of apoE4 can create a nearly 2-fold increase in iNOS levels in a non-aged adult mouse cortical culture, in comparison to apoE3.

Another line of study, pointing to the role of activated microglia in pathology of AD, shows that anti-inflammatory drugs could be a possible treatment for AD. Celastrol, a plant-derived triterpene, decreased the induced expression of class II MHC molecules by microglia and decreased induced NO production in macrophage lineage cells and

endothelial cells [36]. Another study compared postmortem brain tissue from elderly, nondemented, arthritic patients with a history of chronic nonsteroidal anti-inflammatory drug (NSAID) use and nondemented control subjects with no history of arthritis or other condition that might promote the regular use of NSAIDs. In both the NSAID-treated group and control subjects, 59% of patients had some senile plaques, however NSAID use was associated with less microglial activation [37]. These data shows that suppression of microglial activation does not eliminate senile plaques in elderly individuals, however, the role of microglial activation in senile plaque formation at a younger age remains unclear and benefits of anti-inflammatory drugs in AD prevention should be further studied.

Another study examined nitric oxide radical quenching activity of non-steroidal anti-inflammatory drugs and steroidal drugs, using direct *in vitro* nitric oxide radical detecting system by electron spin resonance spectrometry. The non-steroidal anti-inflammatory drugs, aspirin, mefenamic acid, indomethacin and ketoprofen directly and dose-dependently scavenged generated nitric oxide radicals. In experiments of nitric oxide radical donor-induced neuronal damage, these four non-steroidal drugs significantly prevented cell death and apoptotic nuclear changes in neurons [38].

Early detection methods of elevated iNOS or NO production in the brain could be useful biomarkers for detecting apoE4-associated risk for AD. In a recent study, plasma and leukocytes were isolated from 48 sporadic AD and 23 healthy control subjects of same age and sex. The results of that study demonstrate a significant reduction of TGF-beta1 levels in plasma of AD patients and significantly increased NOS activity in leukocytes of AD patients [39].

The results of my study clearly demonstrate that apoE4 induces microglial activation and iNOS production by acting directly on microglia. I propose that elevated iNOS levels, associated with microglial activation in apoE4 individuals may lead to long-term neurotoxicity and, along with shorter neurite outgrowth associated with apoE4, present a second major risk for developing AD. Further study of long-term effects of elevated levels of iNOS and NO on neurons in young and mid-aged adults may give us an insight on the extent to which microglial activation plays a role in AD pathology.

(6) Recently a substantial amount of evidence has emerged on the existence of neurogenesis in the adult brain. These studies have shown proliferation of adult neurons in adult hippocampus [40], dentate gyrus [41] and olfactory bulb [16]. Extent of neurogenesis in adult brain and its role in a normal or injured brain is not yet fully understood.

In the numerous AMC cultures established during my research, in the past two years, neuronal proliferation was observed. However, the AMC culture is grown in medium supplemented from 0 DIV with fibroblast growth factor (FGF) aiding in recovery of neurons after culture preparation. Thus, neuronal proliferation may be attributed to the presence of FGF and not to a naturally occurring event.

It was of interest to determine not only the mechanism of differential regulation of neurite outgrowth by apoE3 and apoE4, but also whether apoE isoforms can regulate neuronal proliferation in the absence of FGF in the cell medium.

Assessment of total cell number in AMC culture treated with apoE3, apoE4 or no apoE (apoE KO) at 4 DIV was performed by using tetrazolium salt (MTT cell proliferation kit), which is cleaved to form a formazan dye by only metabolic active cells.

The formazan dye concentration was then detected by ELISA. At 4 DIV there was no significant difference in cell number between the treatments.

Since AMC cultures are comprised of three major cell types, it was still unclear whether the number of neurons in apoE3, apoE4 or no apoE (apoE KO) treatments at 4 DIV was different. Based on the results of the effect of apoE3, apoE4 and no apoE (apoE KO) on microglial proliferation, results of cell proliferation detected by ELISA could have represented various percentages of metabolically active cell types in each treatment.

Immunocytochemistry for neuron specific β -tubulin followed by the cell count in each treatment showed a slightly higher number of neurons in the apoE3 group, followed by apoE4 and then apoE KO (E3>E4>KO). However, the difference in cell number between three groups at 4 DIV was not significant. Neurons are not fast regenerating cells, which may explain why there was no significant difference in the number of neurons between apoE3 or apoE4 treatment after 2 days of treatment.

Interestingly, no difference was observed in the total number of neurons per cover slip when compared with previous AMC cultures, supplemented with FGF.

To account for the slight but non-significant difference in neuron number in apoE3, apoE4 and no apoE (apoE KO) groups, double immunocytochemistry was performed, anti- β -tubulin and BrdU, which allowed detection of neurons in the DNA synthesis phase. Results of this experiment show (1) the presence of neurons in the DNA synthesis phase in all three treatment groups, (2) approximately 20% of neurons in the DNA synthesis phase in the apoE3 treatment of the total number of neurons treated, (3) 12% in apoE4 treatment and (4) 8% in apoE KO. The percentage of neurons in the DNA synthesis phase in AMC culture treated with apoE3 and no FGF was significantly higher

than such percentage in apoE4 and apoE KO treatments with no FGF. Of note, there was no significant difference between apoE4 and apoE KO treatments.

These data show the evidence for neurogenesis in adult cultured cortical neurons in the absence of growth factors and suggest that apoE plays a role in neurogenesis when compared to no apoE (apoE KO). Furthermore, these data show that apoE3 is more efficient than apoE4 in promoting neurogenesis in AMC culture by 4 DIV. The experiment was performed between 0 and 4 DIV in order to avoid subjecting the cultures to required medium change at 4 DIV. Repeating the experiment for 0-8 DIV may show increased percentages of neurons in the DNA synthesis phase in each treatment.

It is an important finding that helps with better understand the possible roles of apoE isoforms in aging or an injured brain and adds to the evidence of neurogenesis in the adult brain.

Furthermore, another novel finding in this experiment was obtained. Approximately half of the observed BrdU-positive neurons in apoE3, apoE4 and apoE KO treatments exhibited BrdU-positive satellite cell phenomenon. Such phenomenon in spinal ganglia was described previously [42, 43]. It has been shown that satellite cells were young satellite glia, derived from glial progenitor cells.

In my experiments a single BrdU-positive satellite cell was located in the dendritic tree, at the terminal bouton or at perikaryon of approximately half of BrdU-positive neurons in all three treatments. The satellite cell appeared to be of neuronal origin due to the β -tubulin stain detected in satellite cell soma, which lack any membrane extensions.

Previous study [42] has shown that the satellite cell - neuron relationship was formed in spinal ganglia, where satellite cells were tightly connected with perikaryons of some neuroblasts and young neurons. Further study on the role of satellite cells in the dendritic tree or at perikaryon of adult neuron, where both cells are in a DNA synthesis phase, may explain new mechanisms of adult neuronal proliferation.

5. CONCLUSIONS

The aim of the several studies that make up my thesis research was to better understand the mechanism and role of apoE4 in the neuronal environment - in adult mouse cortical culture model. These studies investigated various aspects of membrane, intracellular, and extracellular biology of apoE4 and found five major avenues by which apoE4 may lead to a neurodegenerative diseases, such as AD.

Before I present a summary of the above discussed results, which compare apoE3 and apoE4 functions in adult cortical cultures, I would like to emphasize the importance of apoE to neuronal health regardless of its isoforms, based on the results obtained from the apoE KO group in several studies that comprise my thesis research.

Results show that in the absence of apoE (apoE KO) in AMC culture: (1) neurons are supplied with the lowest amount of lipid, (2) microglia are predominantly (~80%) macrophage-like and fast-proliferating, (3) high level of iNOS is present due to the large number of activated microglia and (4) neurons proliferate slowly; when all of the four outcomes are compared with the presence of either apoE3 or apoE4. These results clearly show that apoE isoforms regulate very important cellular events and play a vital role in adult neuronal biology.

When I compared several functions and mechanisms of apoE3 and apoE4, I found that although the presence of apoE4 is slightly more beneficial to neuronal environment than no apoE, it is far less efficient than the presence of apoE3. When compared to apoE3, apoE4 (1) has slower binding and accumulation rate in adult neurons, (2) delivers fewer lipid to adult neurons and especially neurites, (3) induces microglial activation, proliferation and iNOS production and (4) does not promote neurogenesis. All of these

properties of apoE4, when compared to apoE3, may not lead to acute neuro-degeneration in a young or mid-aged individual with e4 allele(s). However, the long-term accumulated effect may present an accountable risk to aged neurons at the age of 65 and older, resulting in progressive neuronal tissue loss and dementia, found in Alzheimer's disease. Finding agents that may improve apoE4 functions in adult neurons and increase its efficiency to match the efficiency of apoE3 may better protect aged neurons from deterioration.

6. BIBLIOGRAPHY

- [1] Das, H.K., J. McPherson, G.A.P. Bruns, S.K. Karathanasis, and J.L. Breslow. Isolation, characterization, and mapping to chromosome 19 of the human apolipoprotein E gene. *J. Boil. Chem.* (1985) 60:6240-6247.
- [2] Hallman, D.M, E. Boerwinkle, N. Saha, C. Sandholzer, H.J. Menzel, A. Csazar, and G. Utermann. The apolipoprotein E polymorphism: A comparison of allele frequencies and effects in nine populations. *Am. J. Hum. Genet.* (1991) 19:338-349.
- [3] Mahley, R.W. Apolipoprotein E: cholesterol transport protein with expanding role in cell biology. *Science* (1988) 240, 622-30.
- [4] Corder, E.H., A.M. Saunders, W.J. Strittmatter, D.E. Schmechel, P.C. Gaskell, G.W. Small, A.D. Roses, J.L. Haines, and M.A. Pericak-Vance. Gene dose of apolipoprotein E type 4 allele and the risk of Alzheimer's disease in late onset families. *Science* (1993) 261:921-923.
- [5] Nathan BP, Jiang Y, Wong GK, Shen F, Brewer GJ, Struble RG. Apolipoprotein E4 inhibits, and apolipoprotein E3 promotes neurite outgrowth in cultured adult mouse cortical neurons through the low-density lipoprotein receptor-related protein. *Brain Res.* (2002) Feb 22; 928 (1-2): 96-105.
- [6] Pitas RE, Boyles JK, Lee SH, Foss D, Mahley RW. Astrocytes synthesize apolipoprotein E and metabolize apolipoprotein E-containing lipoproteins. *Biochim Biophys Acta.* (1987) Jan 13;917 (1):148-61.
- [7] Katsuse O, Iseki E, Kosaka K. Immunohistochemical study of the expression of cytokines and nitric oxide synthases in brains of patients with dementia with Lewy bodies. *Neuropathology.* (2003) Mar;23 (1):9-15.
- [8] Wegiel J, Imaki H, Wang KC, Wegiel J, Wronska A, Osuchowski M, Rubenstein R. Origin and turnover of microglial cells in fibrillar plaques of APPsw transgenic mice. *Acta Neuropathol (Berl).* (2003) Apr;105 (4):393-402.
- [9] Vehmas AK, Kawas CH, Stewart WF, Troncoso JC. Immune reactive cells in senile plaques and cognitive decline in Alzheimer's disease. *Neurobiol Aging.* (2003) Mar-Apr;24 (2):321-31
- [10] Itagaki S, McGeer PL, Akiyama H. Presence of T-cytotoxic suppressor and leucocyte common antigen positive cells in Alzheimer's disease brain tissue. *Neurosci Lett.* (1988) Sep 12;91 (3):259-64.

- [11] Hartman RE, Laurer H, Longhi L, Bales KR, Paul SM, McIntosh TK, Holtzman DM. Apolipoprotein E4 influences amyloid deposition but not cell loss after traumatic brain injury in a mouse model of Alzheimer's disease. *J Neurosci.* (2002) Dec 1;22 (23):10083-7.
- [12] Pahnke J, Walker LC, Schroeder E, Vogelgesang S, Stausske D, Walther R, Warzok RW. Cerebral beta-amyloid deposition is augmented by the -491AA promoter polymorphism in non-demented elderly individuals bearing the apolipoprotein E epsilon4 allele. *Acta Neuropathol (Berl).* (2003) Jan;105 (1):25-9.
- [13] Dickson DW, Sinicropi S, Yen SH, Ko LW, Mattiace LA, Bucala R, Vlassara H. Glycation and microglial reaction in lesions of Alzheimer's disease. *Neurobiol Aging.* (1996) Sep-Oct;17 (5):733-43.
- [14] Lombardi VR, Garcia M, Cacabelos R., *J Neurosci Res* Microglial activation induced by factor(s) contained in sera from Alzheimer-related ApoE genotypes. (1998) Nov 15;54 (4):539-53
- [15] Garden GA. Microglia in human immunodeficiency virus-associated neurodegeneration. *Glia.* (2002) Nov;40(2):240-51.
- [16] Bridges RS, Grattan DR. Prolactin-induced neurogenesis in the maternal brain. *Trends Endocrinol Metab.* 2003 Jul;14(5):199-201
- [17] Kozorovitskiy Y, Gould E. Adult neurogenesis: a mechanism for brain repair? *J Clin Exp Neuropsychol.* 2003 Aug;25 (5):721-32.
- [18] Mao L, Wang JQ. Adult neural stem/progenitor cells in neurodegenerative repair. *Sheng Li Xue Bao.* 2003 Jun 25;55 (3):233-44.
- [19] McManus DQ, Brewer GJ. Culture of neurons from postmortem rat brain. *Neurosci Lett.* (1997) Mar 21;224 (3):193-6.
- [20] Ji ZS, Dichek HL, Miranda RD, Mahley RW. Heparan sulfate proteoglycans participate in hepatic lipase and apolipoprotein E-mediated binding and uptake of plasma lipoproteins, including high density lipoproteins. *J Biol Chem.* 1997 Dec 12;272 (50):31285-92
- [21] Colton CA, Brown CM, Czapiga M, Vitek MP. Apolipoprotein-E allele-specific regulation of nitric oxide production. *Ann N Y Acad Sci.* (2002) May; 962:212-25
- [22] Bellosta S, Nathan BP, Orth M, Dong LM, Mahley RW, Pitas RE. Stable expression and secretion of apolipoproteins E3 and E4 in mouse neuroblastoma cells produces differential effects on neurite outgrowth. *J Biol Chem.* 1995 Nov 10;270 (45):27063-71.

- [23] Amer RK, Pace-Asciak CR, Mills LR. Neuroscience. A lipoxygenase product, hepxilin A(3), enhances nerve growth factor-dependent neurite regeneration post-axotomy in rat superior cervical ganglion neurons in vitro. 2003;116 (4):935-46.
- [24] Gorio A Ganglioside enhancement of neuronal differentiation, plasticity, and repair. CRC Crit Rev Clin Neurobiol. 1986;2 (3):241-96.
- [25] Ji ZS, Pitas RE, Mahley RW. Differential cellular accumulation/retention of apolipoprotein E mediated by cell surface heparan sulfate proteoglycans. Apolipoproteins E3 and E2 greater than e4. J Biol Chem. 1998 May 29;273 (22):13452-60.
- [26] Mahley RW, Ji ZS. Remnant lipoprotein metabolism: key pathways involving cell-surface heparan sulfate proteoglycans and apolipoprotein E. J Lipid Res. 1999 Jan;40 (1):1-16.
- [27] White F, Nicoll JA, Roses AD, Horsburgh K. Impaired neuronal plasticity in transgenic mice expressing human apolipoprotein E4 compared to E3 in a model of entorhinal cortex lesion. Neurobiol Dis. 2001 Aug;8 (4):611-25.
- [28] Hartman RE, Wozniak DF, Nardi A, Olney JW, Sartorius L, Holtzman DM. Behavioral phenotyping of GFAP-apoE3 and -apoE4 transgenic mice: apoE4 mice show profound working memory impairments in the absence of Alzheimer's-like neuropathology. Exp Neurol. 2001 Aug;170 (2):326-44.
- [29] Sheng H, Laskowitz DT, Bennett E, Schmechel DE, Bart RD, Saunders AM, Pearlstein RD, Roses AD, Warner DS. Apolipoprotein E isoform-specific differences in outcome from focal ischemia in transgenic mice. J Cereb Blood Flow Metab. 1998 Apr;18 (4):361-6.
- [30] Kasurinen J. A novel fluorescent fatty acid, 5-methyl-BDY-3-dodecanoic acid, is a potential probe in lipid transport studies by incorporating selectively to lipid classes of BHK cells. Biochem Biophys Res Commun 1992, 187, 1594-1601
- [31] Colton CA, Brown CM, Cook D, Needham LK, Xu Q, Czapiga M, Saunders AM, Schmechel DE, Rasheed K, Vitek M APOE and the regulation of microglial nitric oxide production: a link between genetic risk and oxidative stress. Neurobiol Aging. 2002 Sep-Oct; 23 (5):777-85.
- [32] Dawson VL, Brahmabhatt HP, Mong JA, Dawson TM. Expression of inducible nitric oxide synthase causes delayed neurotoxicity in primary mixed neuronal-glial cortical cultures. Neuropharmacology (1994) 33 (11):1425-30.
- [33] Arimoto T, Bing G. Up-regulation of inducible nitric oxide synthase in the substantia nigra by lipopolysaccharide causes microglial activation and neurodegeneration. Neurobiol Dis. (2003) Feb;12 (1):35-45.

- [34] Munch G, Gasic-Milenkovic J, Dukic-Stefanovic S, Kuhla B, Heinrich K, Riederer P, Huttunen HJ, Founds H, Sajithlal G. Microglial activation induces cell death, inhibits neurite outgrowth and causes neurite retraction of differentiated neuroblastoma cells. *Exp Brain Res.* (2003) May;150 (1):1-8.
- [35] Katsuse O, Iseki E, Kosaka K. Immunohistochemical study of the expression of cytokines and nitric oxide synthases in brains of patients with dementia with Lewy bodies. *Neuropathology* (2003) Mar;23 (1):9-15.
- [36] Allison AC, Cacabelos R, Lombardi VR, Alvarez XA, Vigo C. Celastrol, a potent antioxidant and anti-inflammatory drug, as a possible treatment for Alzheimer's disease. *Prog Neuropsychopharmacol Biol Psychiatry* (2001) Oct;25 (7):1341-57.
- [37] Mackenzie IR, Munoz DG. Nonsteroidal anti-inflammatory drug use and Alzheimer-type pathology in aging. *Neurology* (1998) Apr;50 (4):986-90.
- [38] Asanuma M, Nishibayashi-Asanuma S, Miyazaki I, Kohno M, Ogawa N. Neuroprotective effects of non-steroidal anti-inflammatory drugs by direct scavenging of nitric oxide radicals. *J Neurochem.* (2001) Mar;76 (6):1895-904.
- [39] De Servi B, La Porta CA, Bontempelli M, Comolli R. Decrease of TGF-beta1 plasma levels and increase of nitric oxide synthase activity in leukocytes as potential biomarkers of Alzheimer's disease. *Exp Gerontol.* (2002) Jun;37 (6):813-21.
- [40] Malberg JE, Duman RS. Cell Proliferation in Adult Hippocampus is Decreased by Inescapable Stress: Reversal by Fluoxetine Treatment. *Neuropsychopharmacology.* 2003 Jul 2
- [41] Jiang W, Wan Q, Zhang ZJ, Wang WD, Huang YG, Rao ZR, Zhang X. Dentate granule cell neurogenesis after seizures induced by pentylenetetrazol in rats. *Brain Res.* 2003 Jul 11; 977 (2):141-8.
- [42] Chumasov EI. Development of satellite-neuron relations in the spinal ganglia of the rat. *Arkh Anat Gistol Embriol.* 1984 Aug;87 (8): 15-22.
- [43] Hall AK, Landis SC Division and migration of satellite glia in the embryonic rat superior cervical ganglion. *J Neurocytol.* 1992 Sep;21(9): 635-47.